



**Report ITU-R RS.2315-0**  
(09/2014)

**Global survey of radio frequency  
interference levels observed by the  
Aquarius scatterometer at 1 260 MHz  
and Aquarius and soil moisture and ocean  
salinity radiometers at 1 413 MHz**

**RS Series**  
**Remote sensing systems**

## Foreword

The role of the Radiocommunication Sector is to ensure the rational, equitable, efficient and economical use of the radio-frequency spectrum by all radiocommunication services, including satellite services, and carry out studies without limit of frequency range on the basis of which Recommendations are adopted.

The regulatory and policy functions of the Radiocommunication Sector are performed by World and Regional Radiocommunication Conferences and Radiocommunication Assemblies supported by Study Groups.

## Policy on Intellectual Property Right (IPR)

ITU-R policy on IPR is described in the Common Patent Policy for ITU-T/ITU-R/ISO/IEC referenced in Annex 1 of Resolution ITU-R 1. Forms to be used for the submission of patent statements and licensing declarations by patent holders are available from <http://www.itu.int/ITU-R/go/patents/en> where the Guidelines for Implementation of the Common Patent Policy for ITU-T/ITU-R/ISO/IEC and the ITU-R patent information database can also be found.

### Series of ITU-R Reports

(Also available online at <http://www.itu.int/publ/R-REP/en>)

Series	Title
<b>BO</b>	Satellite delivery
<b>BR</b>	Recording for production, archival and play-out; film for television
<b>BS</b>	Broadcasting service (sound)
<b>BT</b>	Broadcasting service (television)
<b>F</b>	Fixed service
<b>M</b>	Mobile, radiodetermination, amateur and related satellite services
<b>P</b>	Radiowave propagation
<b>RA</b>	Radio astronomy
<b>RS</b>	<b>Remote sensing systems</b>
<b>S</b>	Fixed-satellite service
<b>SA</b>	Space applications and meteorology
<b>SF</b>	Frequency sharing and coordination between fixed-satellite and fixed service systems
<b>SM</b>	Spectrum management

*Note: This ITU-R Report was approved in English by the Study Group under the procedure detailed in Resolution ITU-R 1.*

*Electronic Publication*  
Geneva, 2015

© ITU 2015

All rights reserved. No part of this publication may be reproduced, by any means whatsoever, without written permission of ITU.

## REPORT ITU-R RS.2315-0

**Global survey of radio frequency interference levels observed  
by the Aquarius scatterometer at 1 260 MHz and Aquarius  
and soil moisture and ocean salinity radiometers at 1 413 MHz**

(Question ITU-R 255/7)

(2014)

TABLE OF CONTENTS

	<i>page</i>
1 Introduction .....	2
1.1 Regulatory situation in the 1215-1 300 MHz frequency band.....	2
1.2 Regulatory situation in the 1 400-1 427 MHz frequency band.....	3
2 Observation of RFI by the Aquarius scatterometer at 1 260 MHz.....	4
2.1 RFI detection .....	6
2.2 RFI source analysis.....	7
2.3 Summary of observed RFI and RFI source analysis .....	7
3 Observation of RFI by Aquarius radiometer in the passive band 1 400-1 427 MHz.....	14
3.1 Description of Aquarius radiometer .....	14
3.2 Global survey of Aquarius radiometer brightness temperature.....	14
4 Observation of RFI by SMOS radiometer in the passive band 1 400-1 427 MHz.....	24
4.1 Description of SMOS Radiometer.....	24
4.2 Approach to improve the SMOS RFI situation .....	26
4.3 Characterisation of the RFI sources.....	27
4.4 Global Survey of RFIs as observed by SMOS radiometer .....	33
4.5 Worldwide evolution of RFI occurrences.....	35
5 Summary of observed RFI and RFI source analysis .....	40

## 1 Introduction

This Report describes the radio frequency (RF) environment experienced by three spaceborne active/passive sensors operating around 1 260 MHz in the Earth exploration-satellite service (EESS) (active) allocation in the 1 215-1 300 MHz band and around 1 413 MHz in the EESS (passive) in the 1 400-1 427 MHz band.

The band 1 215-1 300 MHz is allocated on a primary basis to the radionavigation-satellite service (RNSS) and radiolocation services (RLS) and the band 1 240-1 300 MHz is also allocated on a primary basis to the aeronautical radionavigation service (ARNS). Systems operating under the EESS (active) allocation cannot claim protection from systems operating in the RLS or ARNS in these bands. However, from the perspective of the active sensors operating in the EESS (active), emissions from the terrestrial radars operating in the RLS and ARNS are RF interference (RFI) to these sensors.

The EESS (passive) band 1 400-1 427 MHz is allocated solely for passive operations. The adjacent bands are allocated to the fixed, mobile services and RLS. From the perspective of the passive sensors operating in the EESS (passive), excessive unwanted emissions from the active services in adjacent bands, and unauthorised emissions in the passive band are RFI to these sensors.

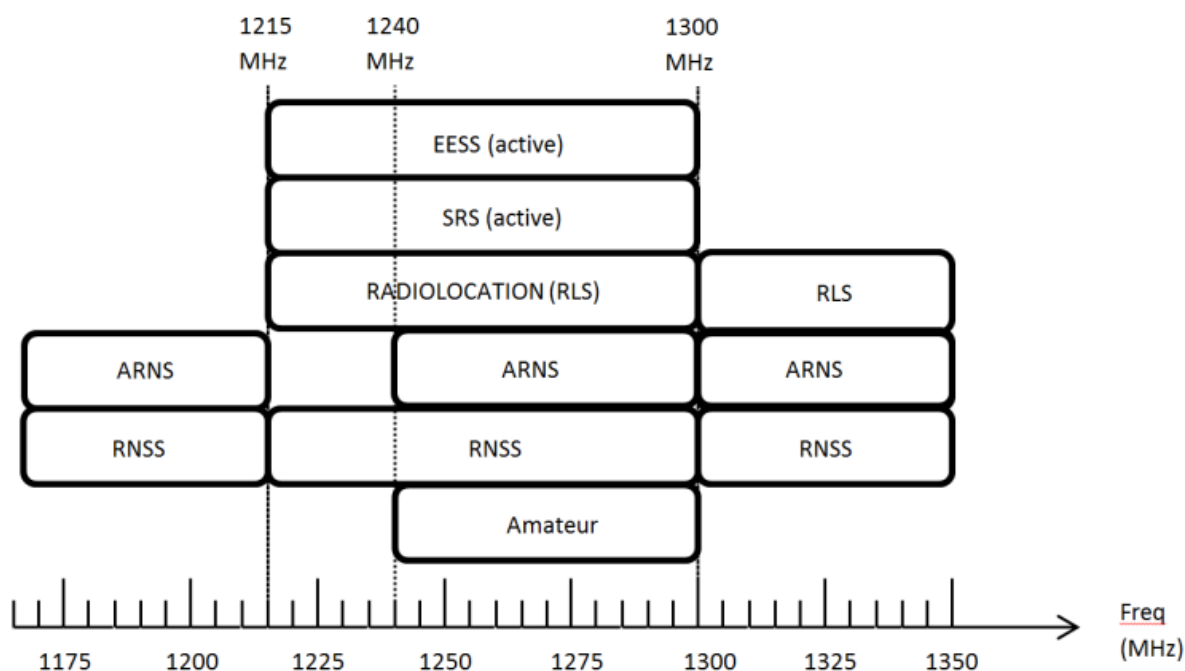
The 7 day global map of RFI power received by the Aquarius scatterometer around 1 260 MHz is presented. Presented for comparison is the RF environment for the Aquarius radiometer in a 7 day global map of brightness temperature for the same 7 day period as for the scatterometer. Also the global map of brightness temperature and RFI probability for the soil moisture and ocean salinity (SMOS) radiometer are presented. This document describes RFI as measured by three spaceborne active/passive sensors. Such information may be useful for the design of future spaceborne active/passive sensors in these bands.

### 1.1 Regulatory situation in the 1 215-1 300 MHz frequency band

The 1 215-1 300 MHz band is allocated on a primary basis to the EESS (active) with constraints given in ITU-R Radio Regulations (RR) No. **5.332** in the 1 215-1 260 MHz sub-band, Nos. **5.332** and **5.335** in the 1 240-1 300 MHz sub-band and No. **5.335A** in the 1 260-1 300 MHz sub-band. RR No. **5.332** states that “In the band 1 215-1 260 MHz, active spaceborne sensors in the Earth exploration-satellite and space research services shall not cause harmful interference to, claim protection from, or otherwise impose constraints on operation or development of the radiolocation service, the radionavigation-satellite service and other services allocated on a primary basis.” RR No. **5.335** states that “In Canada and the United States in the band 1 240-1 300 MHz, active spaceborne sensors in the Earth exploration-satellite and space research services shall not cause interference to, claim protection from, or otherwise impose constraints on operation or development of the aeronautical radionavigation service.” RR No. **5.335A** states that “In the band 1 260-1 300 MHz, active spaceborne sensors in the Earth exploration-satellite and space research services shall not cause harmful interference to, claim protection from, or otherwise impose constraints on operation or development of the radiolocation service and other services allocated by footnotes on a primary basis.” Since EESS (active) cannot claim protection from the radiolocation service, the aeronautical radionavigation service nor the radionavigation-satellite service in these respective sub-bands, EESS (active) systems has to mitigate the RFI received by these other primary services. Figure 1 shows the ITU-R frequency allocations in and around the 1 215-1 300 MHz frequency range.

Below the 1 215-1 300 MHz band allocated to EESS (active) is the 1 164-1 215 MHz band which is allocated on a primary basis to the ARNS and the RNSS (space-to-Earth) (space-to-space). Above the 1 215-1 300 MHz band is the 1 300-1 350 MHz band which is allocated on a primary basis to the RLS, the ARNS and the RNSS (space-to-Earth).

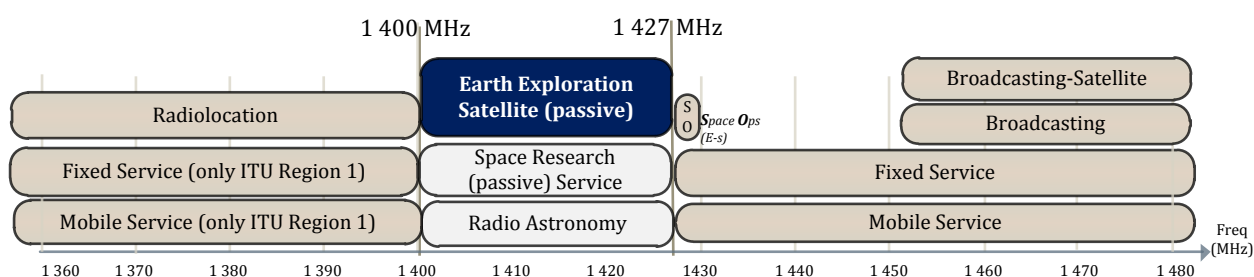
FIGURE 1  
ITU-R frequency allocations in the 1 215-1 300 MHz range and adjacent frequency bands



## 1.2 Regulatory situation in the 1 400-1 427 MHz frequency band

The band 1 400-1 427 MHz is allocated on a primary basis to the EESS (passive), SRS (passive) and to the radio astronomy service as shown in Fig. 2. All emissions are prohibited in this band according to ITU-R RR No. **5.340**. In addition, WRC-07 adopted Resolution **750** on the compatibility between the EESS (passive) and relevant active services. Concerning the 1 400-1 427 MHz band, ITU-R Resolution **750** contains the recommended maximum levels of unwanted emissions from active service stations within the EESS (passive) band applicable to the ITU-R services allocated in the adjacent bands. This Resolution also resolves to urge administrations to take all reasonable steps to ensure that unwanted emissions of active services do not exceed the specific recommended maximum levels, noting that EESS passive sensors provide worldwide measurements that benefit all countries.

FIGURE 2  
ITU-R frequency allocations in the 1 400-1 427 MHz range and adjacent frequency bands



The evidence of RFI levels that prevent geophysical measurements is the rationale for having compulsory (not only recommended) limits to protect the purely passive bands. In Europe, the CEPT Electronic Communications Committee (ECC) approved in March 2011 a new decision

ECC/DEC/(11)01 on the protection of the EESS (passive) service in the 1 400-1 427 MHz band. This ECC decision, which was proposed with the support of ESA, CNES, ANFR, and EUMETNET, translates the compatibility criteria recommended by ITU into mandatory limits and intends to give a clear signal to the international community about the recognition by CEPT of the societal and economical values of the EESS (passive) applications related to climate change and natural disasters prediction.

The limits for unwanted emissions apply to stations in the active services operating in CEPT countries in the 1 350-1 400 and 1 427-1 452 MHz bands brought into use after 1 January 2012. Each CEPT administration decides on the implementation of the ECC decision. By October 2014, 18 European countries have already implemented this decision, and the implementation is planned in 7 countries. SMOS, AQUARIUS, SMAP and other future Earth observation (EO) missions operating in the 1 400-1 427 MHz passive band, will benefit from this decision.

Further information about this CEPT ECC decision is available at:

<http://www.erodocdb.dk/Docs/doc98/official/pdf/ECCDEC1101.PDF>

[http://www.erodocdb.dk/doks/implement\\_doc\\_adm.aspx?docid=2398](http://www.erodocdb.dk/doks/implement_doc_adm.aspx?docid=2398)

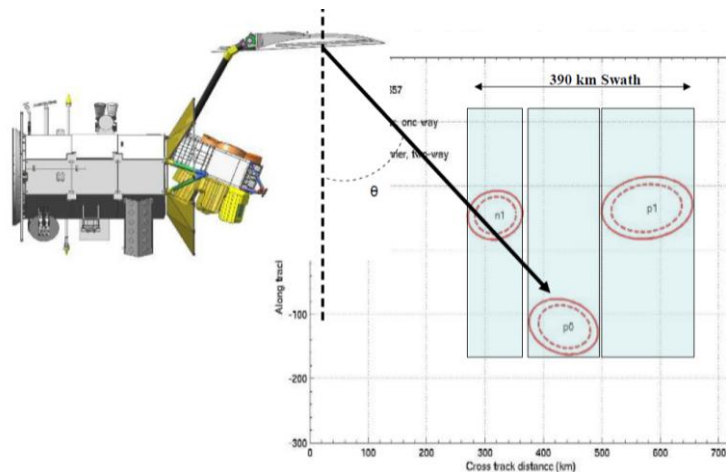
To increase the awareness of the impact of RFI in the passive sensors, the SMOS RFI issue was brought to the attention of the European Commission, who underlined the importance of strengthening the co-operation of all EU member states in the investigation of the RFI sources over their territories. (See EC Doc. Ref. EC RSCOM10-34 (2010)).

## **2 Observation of RFI by the Aquarius scatterometer at 1 260 MHz**

Aquarius is a microwave remote sensing instrument designed to obtain global maps of the surface salinity field of the oceans from space, and it is flown on the Aquarius/Satélite de Aplicaciones Científicas-D (SAC-D) mission, a partnership between the USA National Aeronautics and Space Administration (NASA) and Argentina Comisión Nacional de Actividades Espaciales (CONAE). Aquarius was successfully launched in June 2011. The Aquarius instrument is a combination scatterometer and radiometer operating at 1.26 GHz for the scatterometer (active sensor) and at 1.413 GHz for the radiometer (passive sensor). Even though the primary instrument for measuring salinity is the radiometer which responds to salinity because of the modulation salinity produces on thermal emission from sea water, the scatterometer provides a correction for surface roughness (waves) which is one of the greatest unknowns in the retrieval.

The Aquarius scatterometer maps the world every 7 days. The Aquarius scatterometer is a 1.26 GHz, total power scatterometer designed to acquire radar backscatter signals to estimate ocean-surface roughness. The spaceborne scatterometer operates at an altitude of 657 km and inclination of 98 degrees. The Aquarius scatterometer, co-points with the primary radiometer subsystem, to actively estimate ocean roughness and enable this temperature correction. The radar scatterometer collects fully polarimetric returns and they are summed to represent the total ocean backscatter. The range bandwidth is 4 MHz. The linearly frequency modulated (FM) pulses have a pulse duration of 1 millisecond and bandwidth of 4 MHz. Three beams from an offset – parabolic reflector provide a 280 km width swath. The 2.9 m × 2.5 m offset parabolic reflector with three feeds produces inner, middle and outer 3 dB beam widths of 6.5 degrees, 6.7 degrees, and 7.1 degrees, respectively. An illustration of the three beams of the Aquarius scatterometer and the three footprints on the Earth is shown in Fig. 3. Each of the three beams is pointed at different nadir angles in order for the footprints to cover 390 km across track on the ground. The radar cycles among the three beams every 60 ms.

FIGURE 3  
Illustration of three footprints of three antenna beams of Aquarius scatterometer



Following the June 2011 launch and activation of the Aquarius instrument, RFI was observed to be present globally in the Aquarius scatterometer band 1 258-1 262 MHz. Onboard RFI flagging was available but is not sufficient for removing RFI effects for further processing, so an RFI detection and filtering algorithm was developed for ground data processing. Most RFI over the ocean has been effectively removed, and a substantial amount of RFI has been removed over most land areas. The global survey maps of observed RFI at 1 260 MHz herein shows that certain land areas are contaminated with RFI.

The Aquarius scatterometer radar alternates horizontal (H) and vertical (V) transmit and receive polarized pulses, and interleaves noise-only measurements on each polarization. The echo data has HH, VV, HV, and VH transmit-receive polarizations, and  $nH$  and  $nV$  noise-only receive polarizations. During every other  $nV$  measurement, a noise diode injects a signal into the receive path which raises the apparent  $nV$  noise floor. Figure 4 shows the timing sequence of the Aquarius instrument. Figure 5 is a map of the V-pol and H-pol noise-only receive channels over a 7-day global mapping period. There are regions of high RFI in eastern North America, Europe, and East Asia, with numerous other high RFI regions in other land areas.

These global RFI maps show several types of RFI coupling: 1) the main beam of a ground radar entering the sidelobes of the Aquarius scatterometer, and 2) ground radar sidelobes entering one of the Aquarius radar main beams. The first type of RFI coupling is apparent as far as 3 000 km from the RFI source and into the nearby oceans. This coupling type usually appears simultaneously in all 3 radar beams. The second type of RFI coupling appears at the location of the RFI source and usually shows up in only one of the 3 beams at one time.

FIGURE 4  
Timing sequence of Aquarius instrument

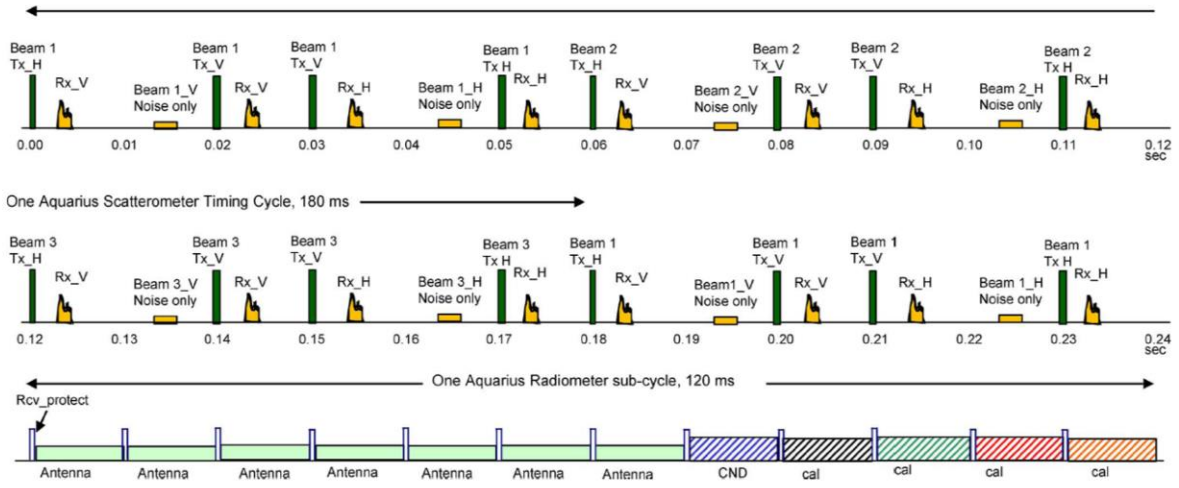
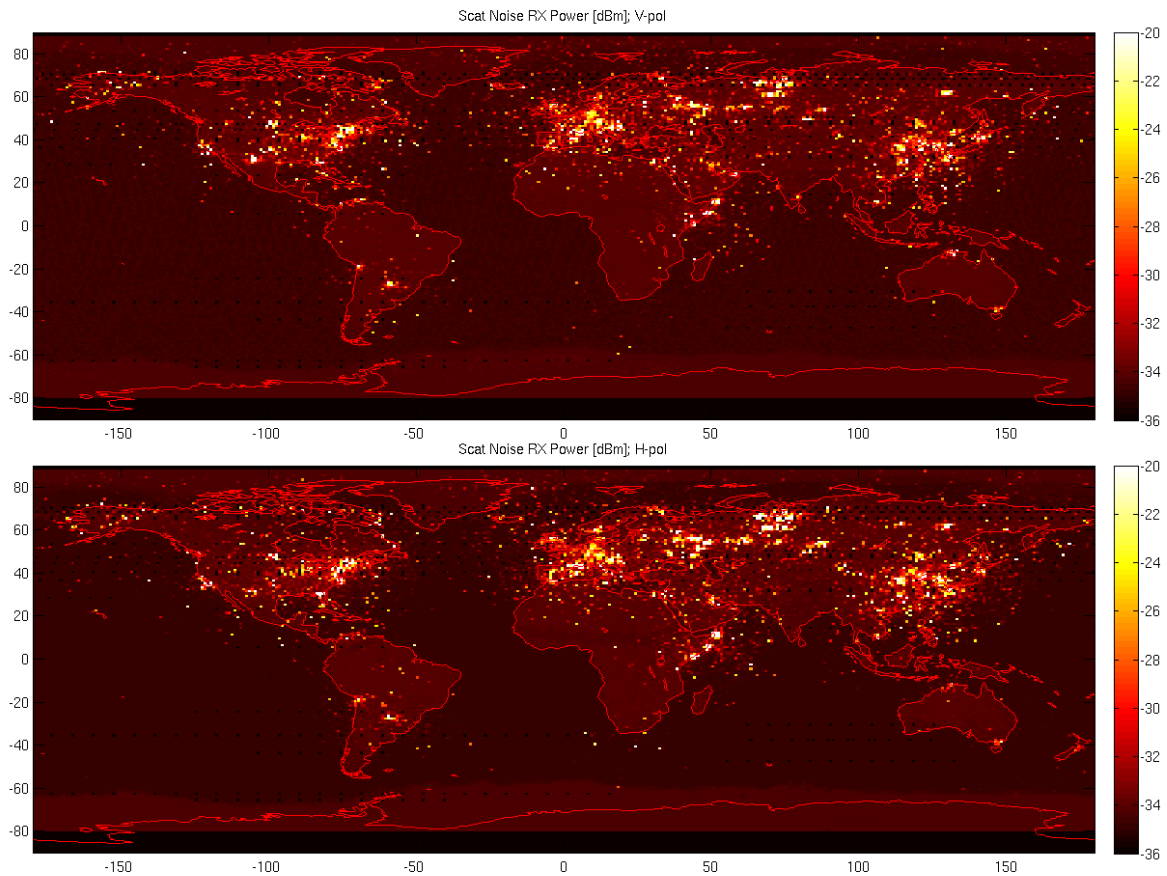


FIGURE 5  
Global map of RFI into Aquarius scatterometer at 1 260 MHz



### 2.1 RFI detection

The onboard RFI detection algorithm uses a threshold level of the high-rate 16 MHz digital sampling. Any pulsed RFI from ground sources are integrated over the Aquarius 2 ms receive windows. The scatterometer has thresholds at the RF front-end and at the analog-to-digital converter (ADC) input.



## 2.2 RFI source analysis

Individual RFI sources can be identified from the Aquarius scatterometer RFI data using the spatial and temporal resolution. The observed RFI effects can be compared with the predicted RFI effects.

Figure 6 shows RFI power values over North America when the cumulative distribution function (CDF) equals to 90.0 to 100%, using histograms of noise received power in every  $1 \times 1$  degree grid cell, and from histograms, the probability distribution functions (PDFs) and CDFs for every  $1 \times 1$  degree grid cell. The RFI maps are shown for H-pol in the top row and for V-pol in the bottom row. For example, in the top left is a map of the H-pol receive noise power value such that for each cell, 90.0% of the data in the cell is less than this value (color coded using values from color bar). It seems to be easier to identify the location of sources of RFI for lower CDF values around 99.5%. Figure 7 shows an example of identifying the locations of Aquarius high localized RFI areas with nearby air traffic control (ATC) radars over North America. Figure 8 shows a complementary cumulative distribution curve (1-CDF) of RFI levels observed January-March 2013 for the continental U.S.

The receiver gain from the antenna feeds to the ADC input is about 67 dB, so for example if the RFI level is  $-10$  dBm at the ADC input, then the signal level at the antenna feeds is  $-76$  dBm, or  $-106$  dBW. Figures 9, 10 and 11 show the RFI maps of the maximum observed noise in ITU Regions 1, 2 and 3, respectively. By comparing the weekly RFI maps of the maximum observed noise, it is possible to see new sources of RFI as in Fig. 12 for the northern part of Region 2. It is also possible to see RFI sources disappear by comparing the weekly RFI maps of the maximum observed noise, as in Fig. 13 for the southern part of Region 1.

The expected RFI signal levels generated from RFI and source/receiver modeling can be compared to the RFI levels Aquarius actually observes. Analyses like these can aid in studies of RFI effects on future L-band satellite missions, and in studying the terrestrial L-band RFI environment as it evolves in the near future. Because of the reciprocity of the antenna gains, the observed RFI levels into the Aquarius scatterometer can be used to estimate the RFI levels into the ground radars from the spaceborne radar.

## 2.3 Summary of observed RFI and RFI source analysis

Within this paper have been presented RFI as observed globally by the Aquarius scatterometer at 1 260 MHz. Examples are given of how these data can be used for RFI source analysis.

FIGURE 6  
 Maps of RFI into Aquarius scatterometer over North America for H-pol  
 and V-pol Data for 90% to 100%

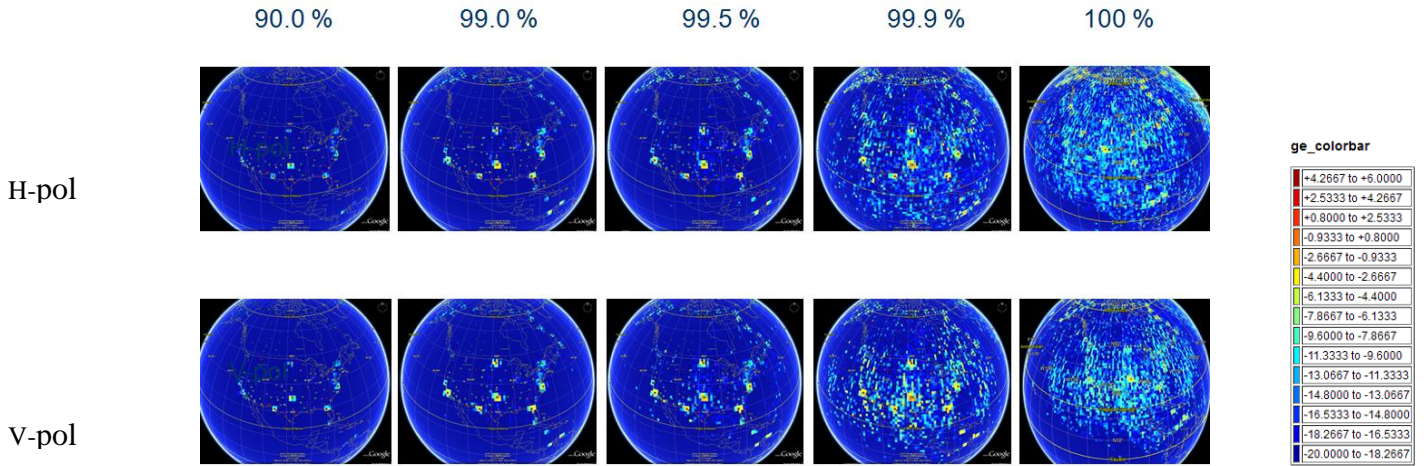


FIGURE 7  
 Aquarius-determined high RFI localized areas in North America  
 identified with ATC radars

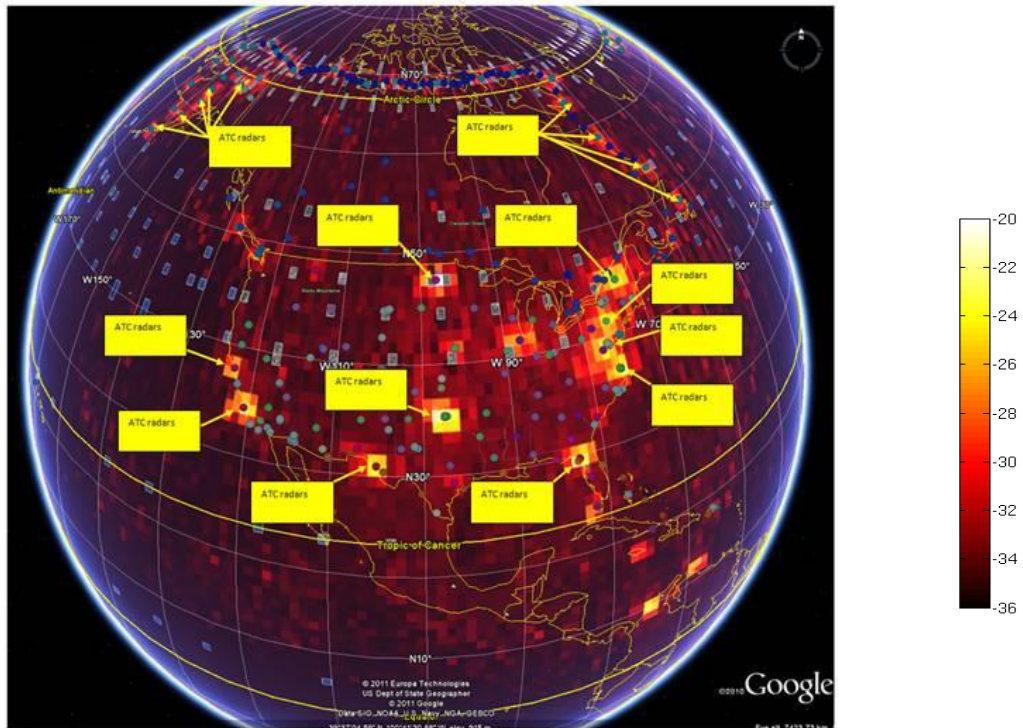


FIGURE 8  
1-CDF distribution of observed noise power at scatterometer ADC input for  
North America (Jan-Mar 2013)

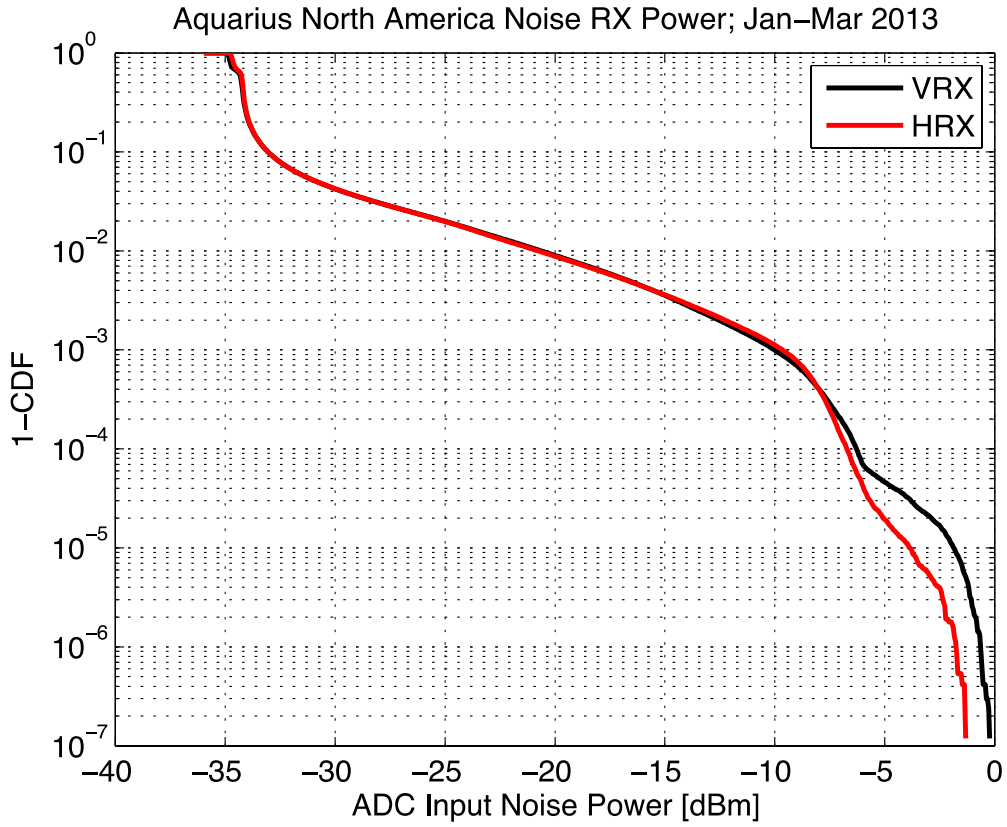


FIGURE 9

Map of observed maximum noise power at ADC input for Europe and Northern Africa (Region 1)

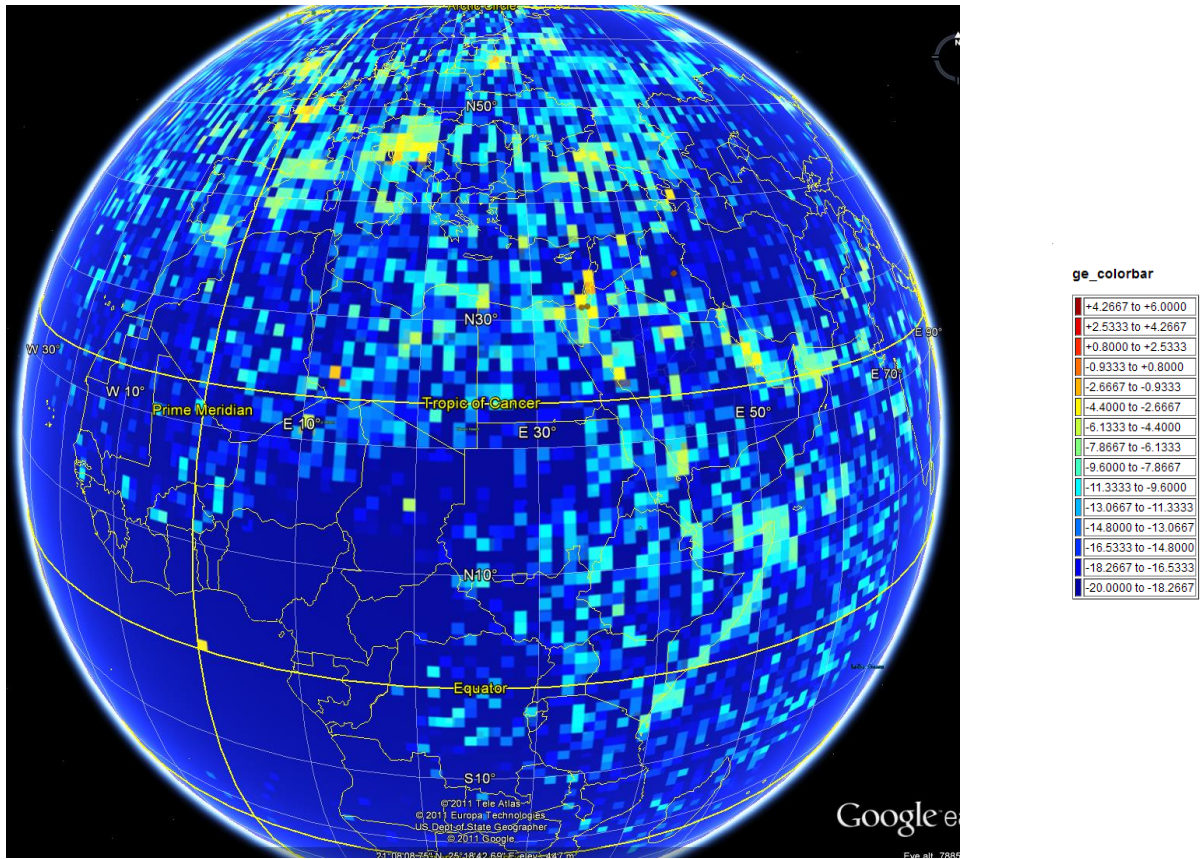


FIGURE 10

Map of observed maximum noise power at ADC input for North America (Region 2)

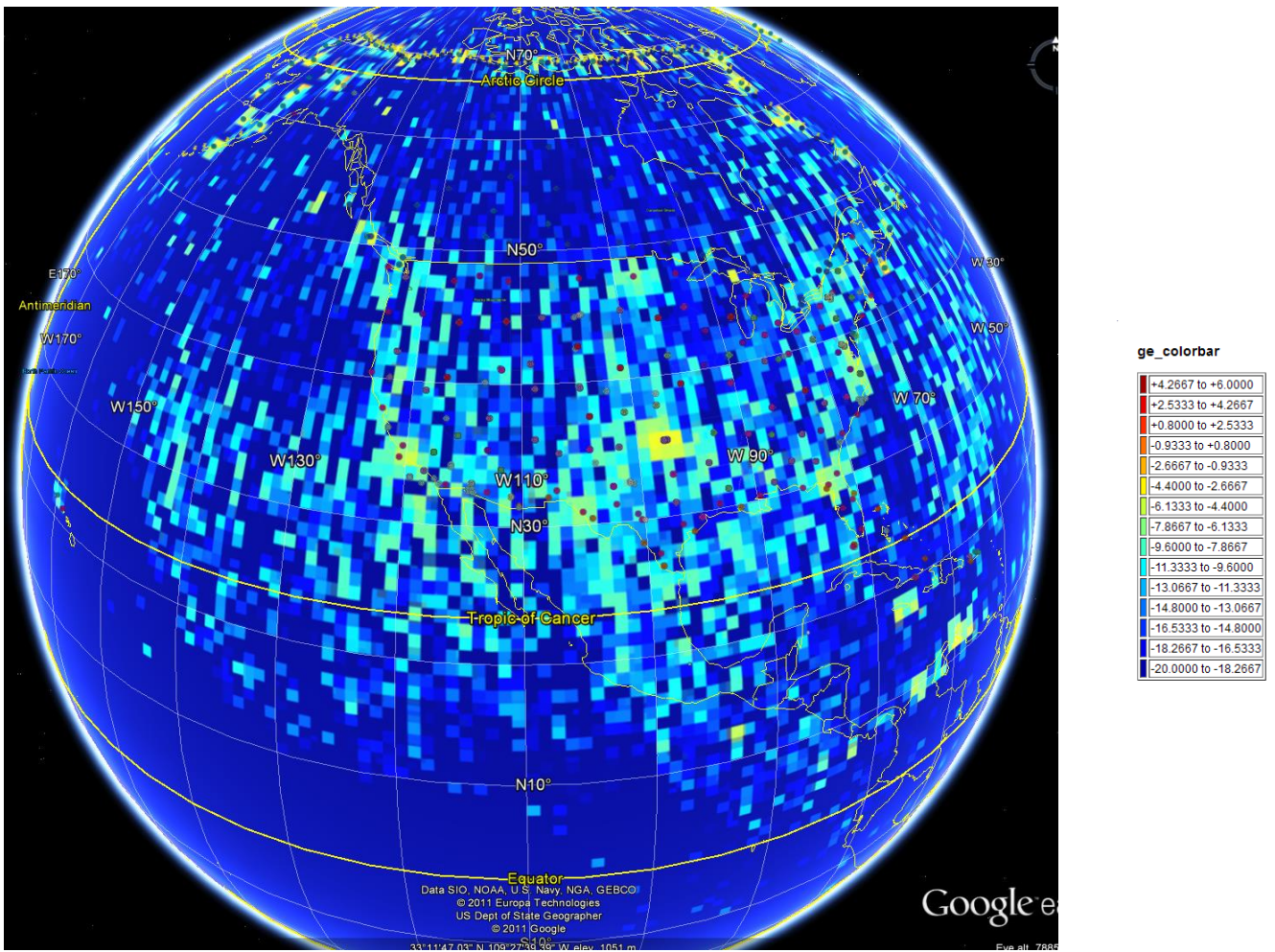


FIGURE 11

Map of observed maximum noise power at ADC input for Asia-Pacific (Region 3)

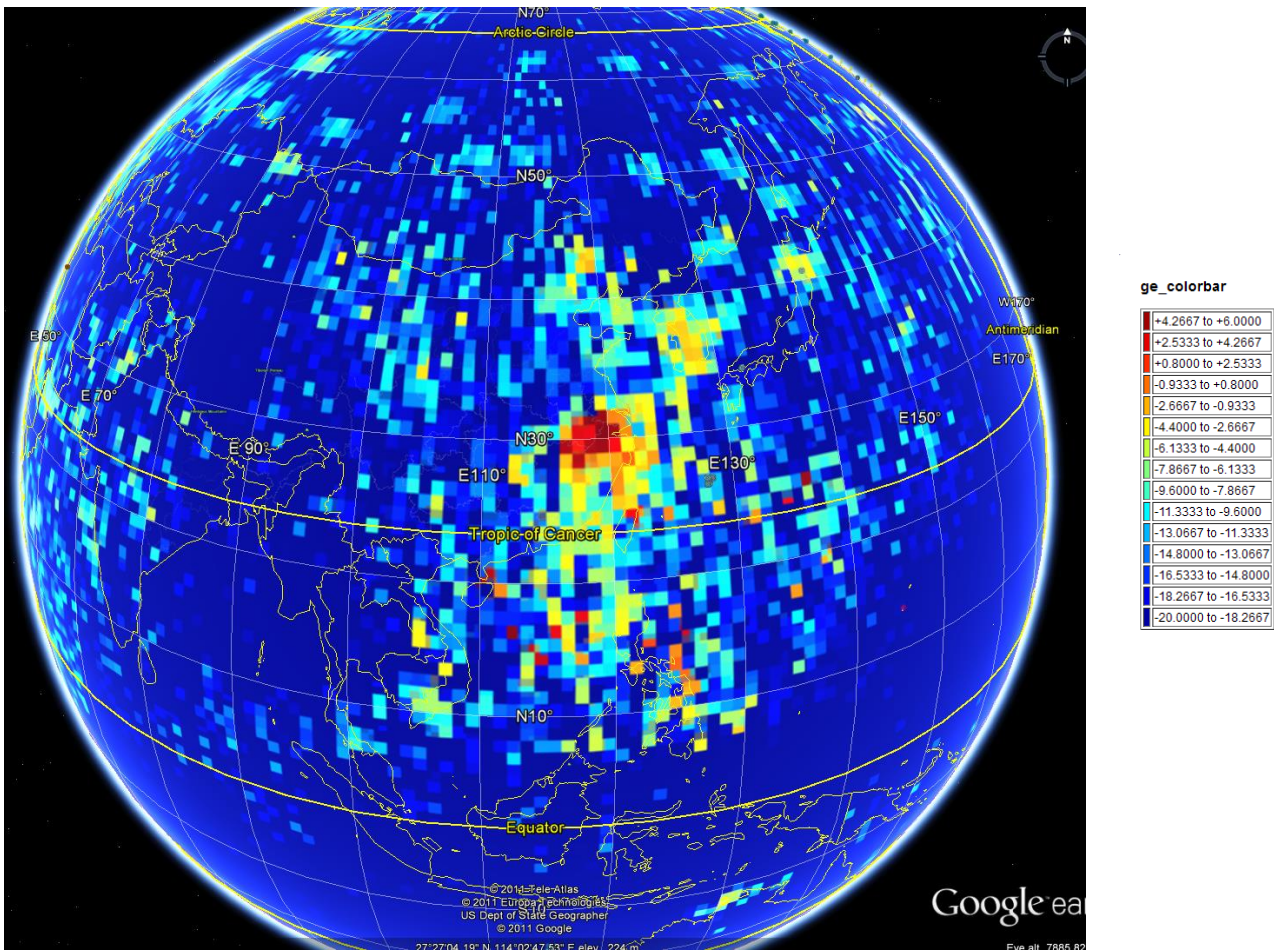
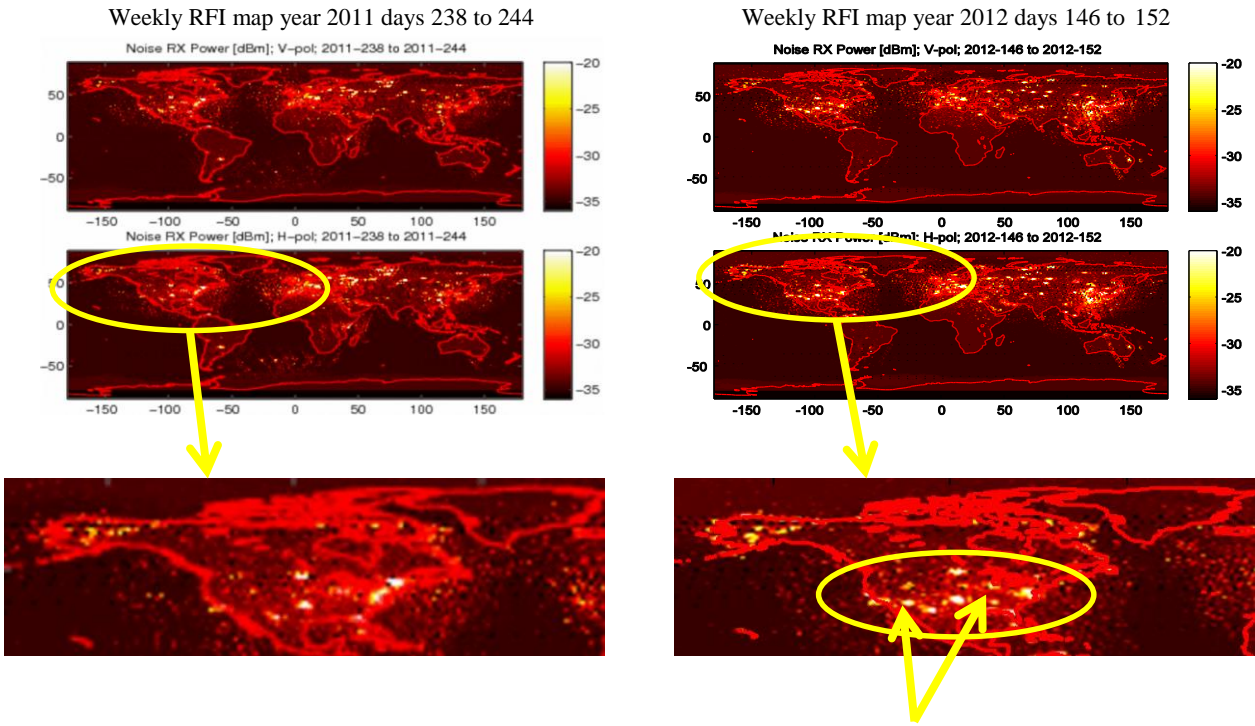
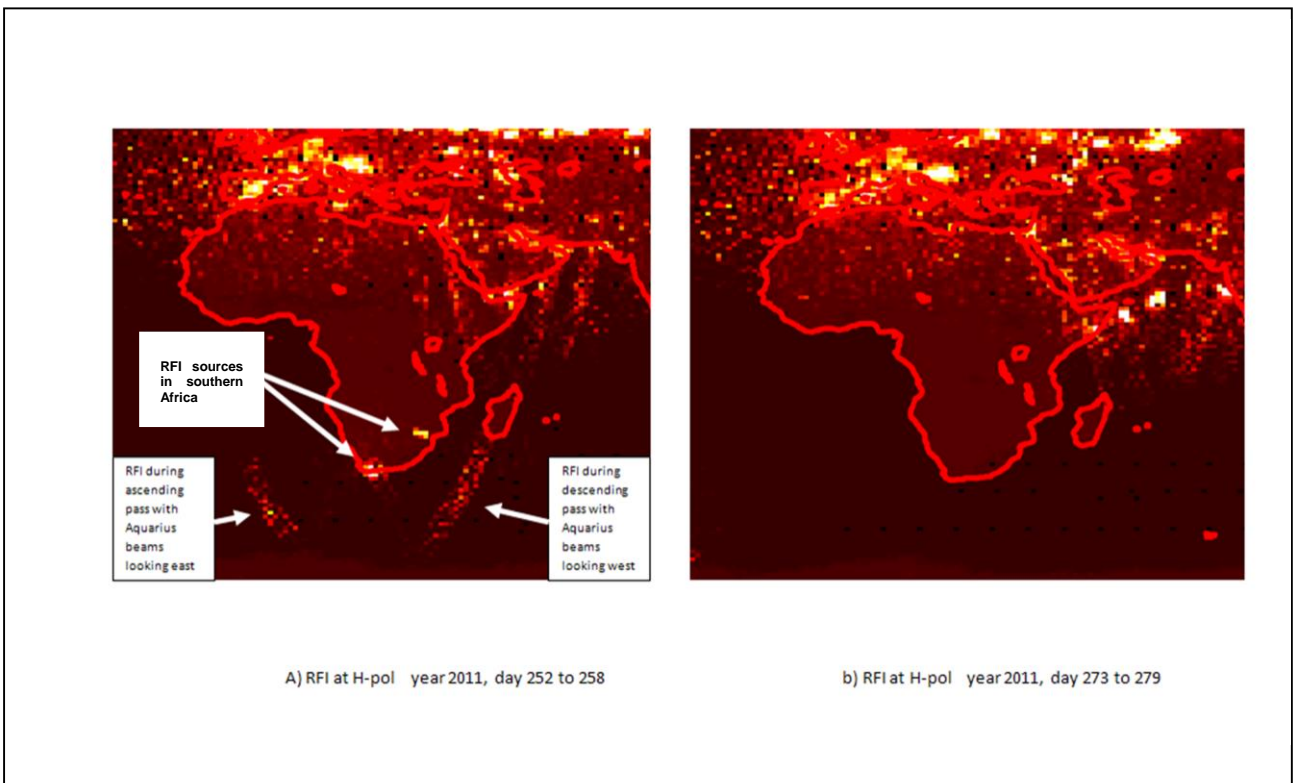


FIGURE 12  
Comparison of observed weekly maximum noise power at ADC input  
in 2011 and 2012 for the northern part of Region 2



NOTE – Weekly RFI map shows additional RFI sources by comparing observed RFI in days 238-244/2011 to that in days 146-152/2012.

FIGURE 13  
Comparison of observed weekly maximum noise power at ADC input  
in 2011 two weeks apart for the southern part of Region 1



### 3 Observation of RFI by Aquarius radiometer in the passive band 1 400-1 427 MHz

#### 3.1 Description of Aquarius radiometer

The Aquarius radiometer maps the world every 7 days. The radiometer has adequate internal calibration and good thermal control. It uses two internal reference sources (noise diode and Dicke load). The primary amplification is done in the receiver front ends (RFEs). There is a separate RFE for each feed assembly. In the RFE, the two signals from the orthomode transducer (OMT) (one for vertical polarization and one for horizontal polarization) are amplified and then combined to form four channels (vertical, horizontal, and the sum and difference of each). The sum and difference signal are used to compute the third Stokes parameter (i.e. detected with a square-law detector in the RFE and later subtracted during the ground processing). The first elements at the input of the RFE are the Dicke switch and its reference load followed by a coupler to a noise diode that provides the hot load. Together, these are the references used for internal calibration. The radiometric temperature of the Dicke load must be known with an uncertainty of <50 mK and the coupled noise temperature must be stable to < 300 ppm, adequate to achieve the required radiometric stability (0.13 K over 7 days). In addition, this radiometer architecture is largely implemented using microstrip-based technology, which is a trade-off made to reduce size and improve thermal control at the expense of increased loss. As with the scatterometer which shares the antennas with the radiometer, the three beams from an offset parabolic reflector provide a 390 km width swath. The 2.9 m × 2.5 m offset parabolic reflector with three feeds produces inner, middle and outer 3 dB beam widths of 6.1 degrees, 6.2 degrees and 6.4 degrees, respectively.

The Aquarius radiometer returns brightness measurements over most of the Earth, including land and ice as well as ocean areas. As far as timing for the hardware, the fundamental timing unit is 10 ms (approximately 1 ms for the scatterometer transmit pulse and 9 ms of observation time for the radiometer). The radiometer and scatterometer operations are alternated so that the two sensors look at the same piece of ocean nearly simultaneously. The three radiometers (one for each beam) operate in parallel. During 120 ms, each radiometer collects seven samples (9 ms long and repeated each 10 ms) looking into the antenna followed by five samples devoted to the calibration sources (two noise diodes and Dicke load). This 120-ms sequence is then repeated. However, because of limitations with the onboard data storage, the radiometer cannot download all of these data. The first and second 10 ms antenna looks are averaged together, as are the third and fourth. The next three antenna looks are left at the 10-ms resolution. The samples of the calibration references transmitted to the ground are the average of ten samples.

#### 3.2 Global survey of Aquarius radiometer brightness temperature

The Aquarius radiometer operations are alternated so that the two sensors look at the same piece of ocean nearly simultaneously as illustrated in Fig. 4 which shows the timing sequence of the Aquarius instrument. Figure 14 is a complementary CDF plot (1-CDF) of the radiometer brightness temperature (BT) in dB K, as observed over North America during January-March 2013. Figures 15, 16 and 17 show the RFI maps of the maximum BT in dB K in Regions 1, 2, and 3, respectively. Figure 18 is a global map of the radiometer BT over a 7-day global mapping period. The white patches indicate missing data. The scatterometer RFI levels are shown in a global map over the same 7-day mapping period. Figure 19 shows 7-day global maps of observed RFI by the scatterometer and radiometer with three months intervals. Both the radiometer BT map and the scatterometer RFI level map show that there are regions of high RFI in eastern North America, Europe, and East Asia, with numerous other high RFI regions in other land areas.



FIGURE 14  
CDF distribution of observed BT at radiometer input for  
North America (Jan-Mar 2013)

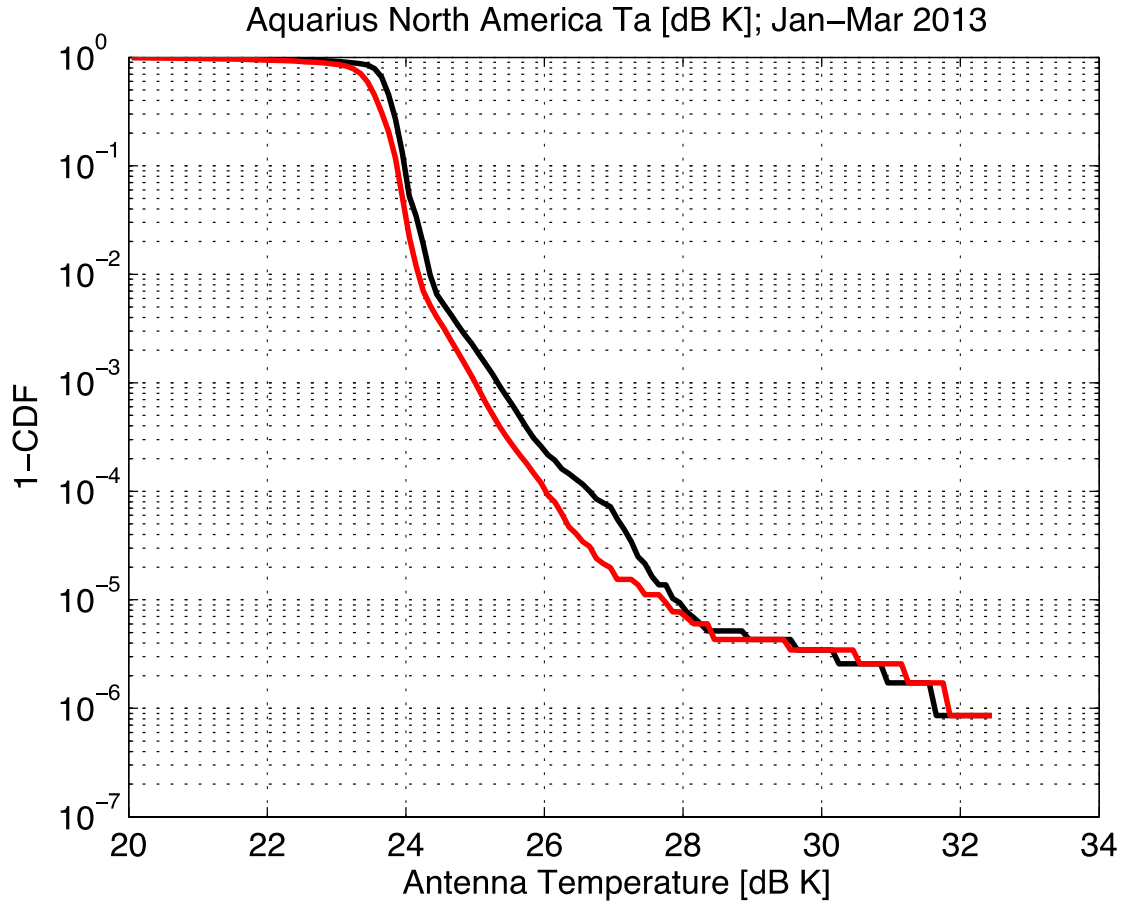


FIGURE 15  
 Map of observed BT at radiometer input for  
 Europe and Northern Africa (Region 1)

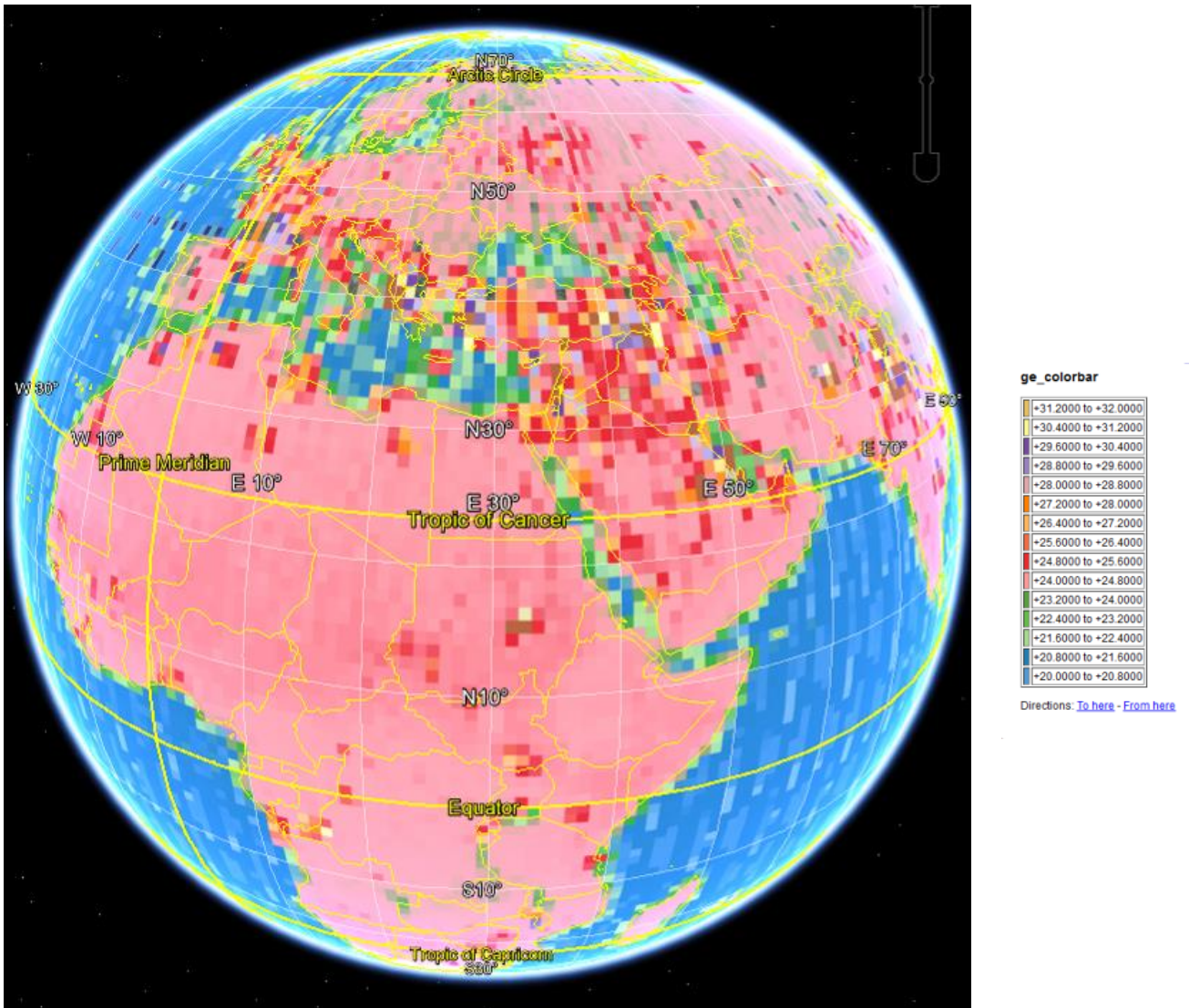


FIGURE 16  
Map of observed BT at radiometer input for  
North America (Region 2)

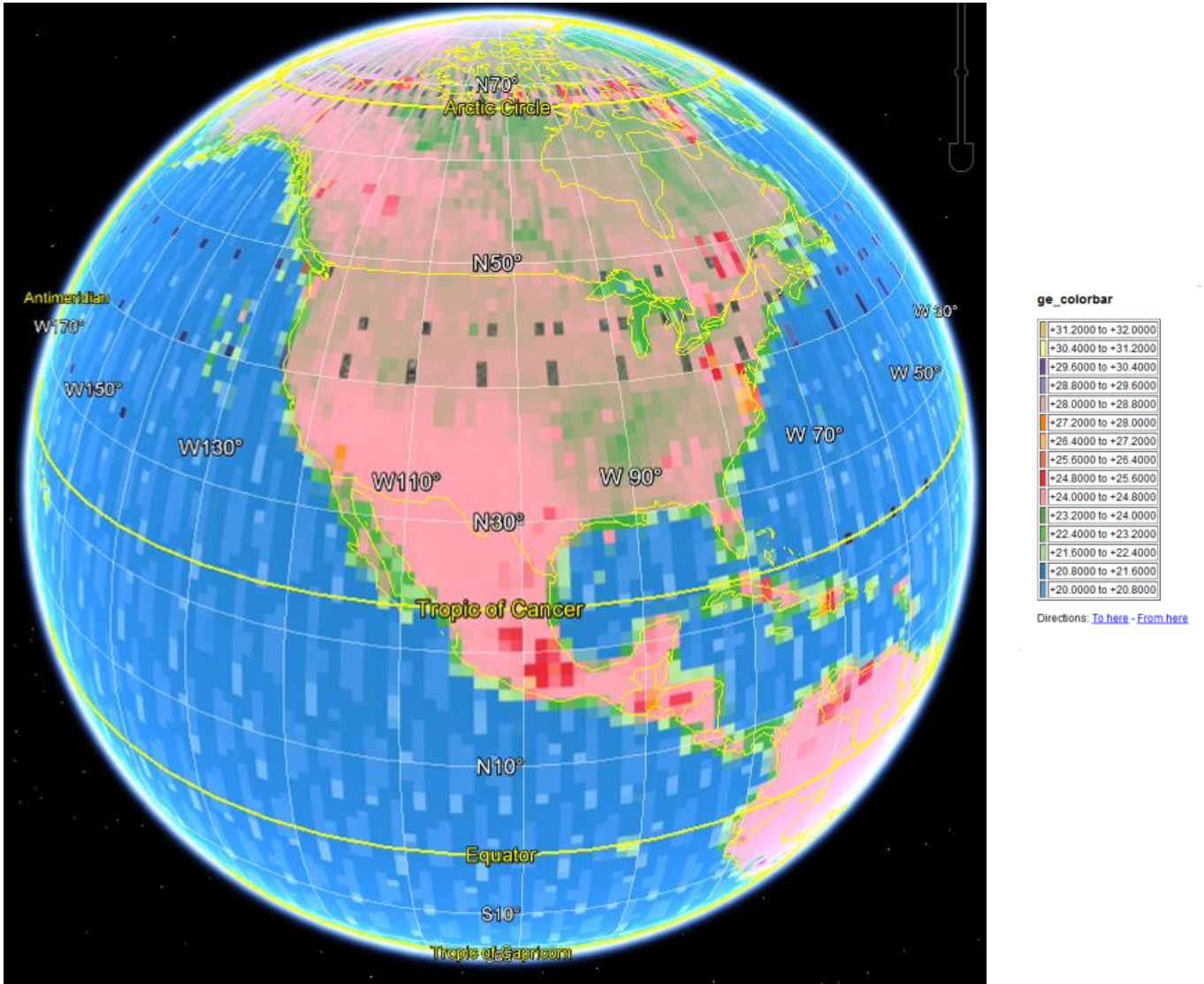


FIGURE 17

Map of observed BT at radiometer input for Asia-Pacific (Region 3)

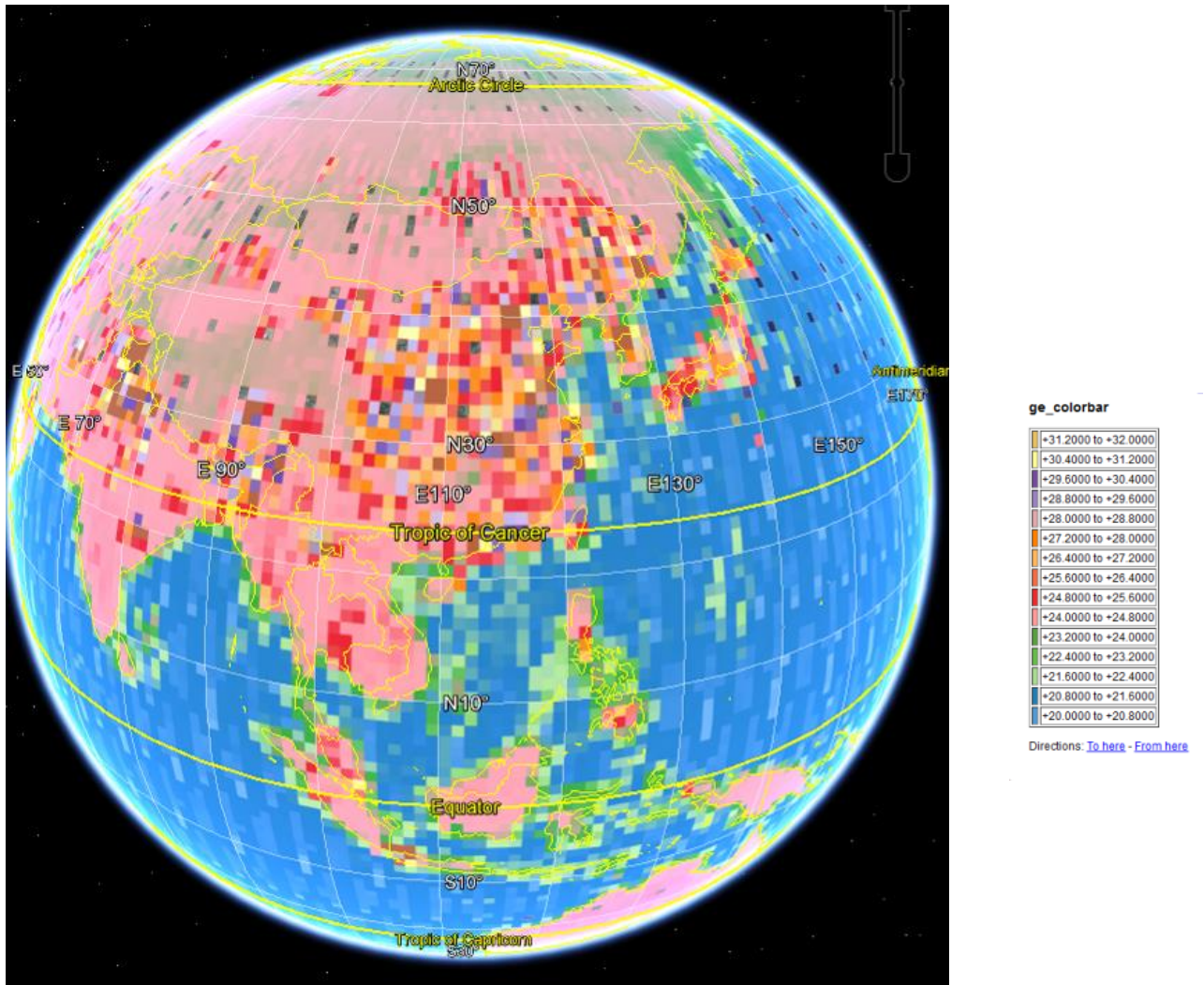
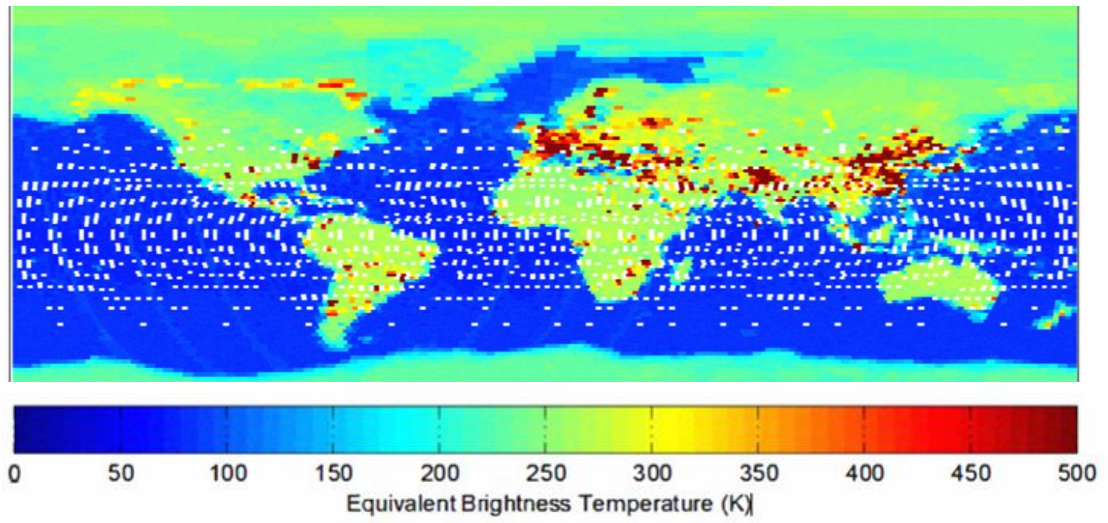


FIGURE 18

Comparison of Aquarius instrument observed weekly radiometer BT and scatterometer maximum noise power at ADC input for same one-week period

a) Observed 7-day radiometer BT



b) Observed 7-day scatterometer maximum noise power

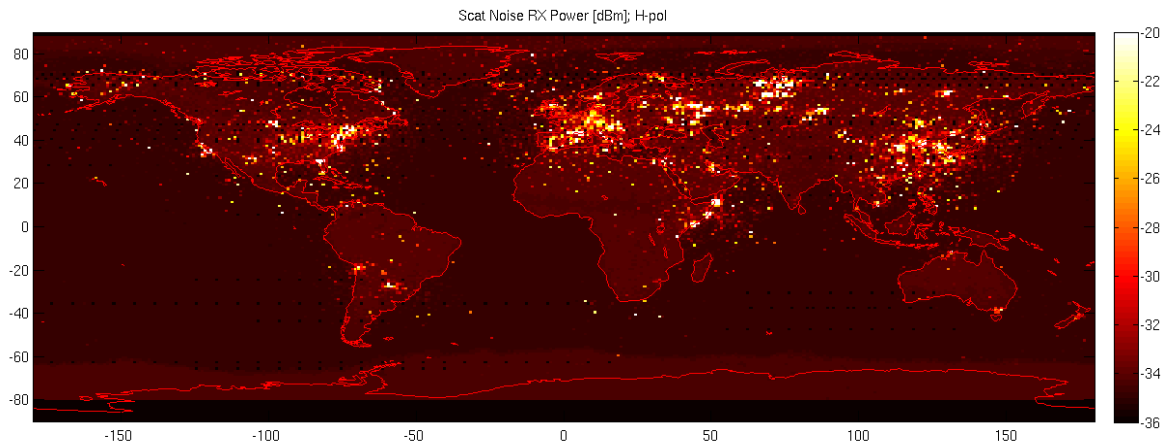
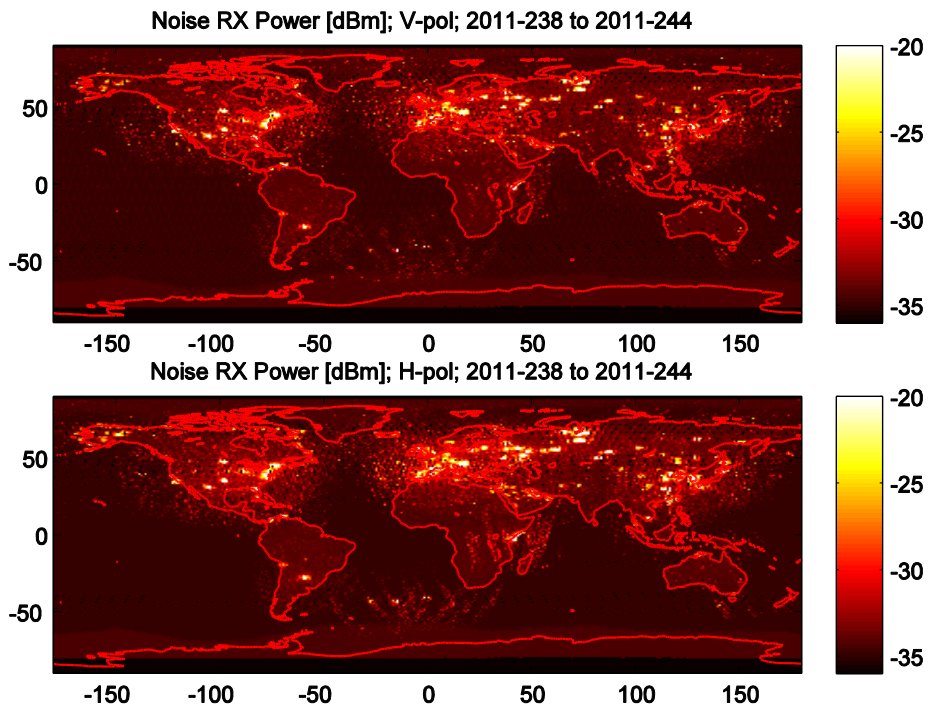


FIGURE 19

Global maps of Aquarius scatterometer and radiometer RFI

a) Aquarius scatterometer receiver noise power 2011-238 to 244



b) Aquarius radiometer BT 2011-238 to 244

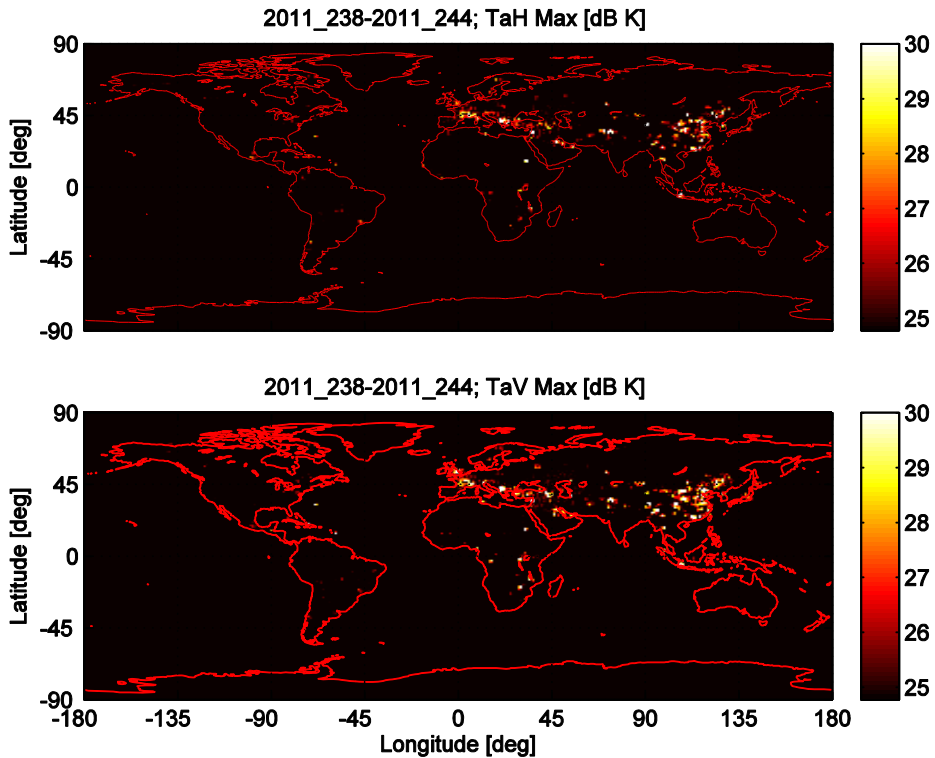
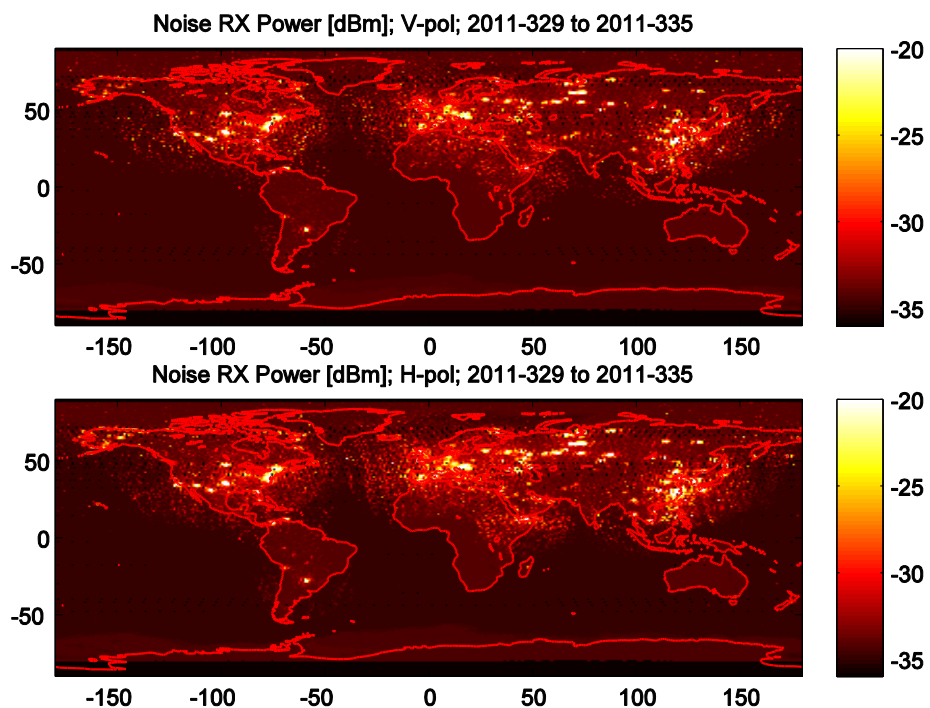


FIGURE 19 (cont.)

Global maps of Aquarius scatterometer and radiometer RFI

c) Aquarius scatterometer receiver noise power 2011-329 to 335



d) Aquarius radiometer BT 2011-329 to 335

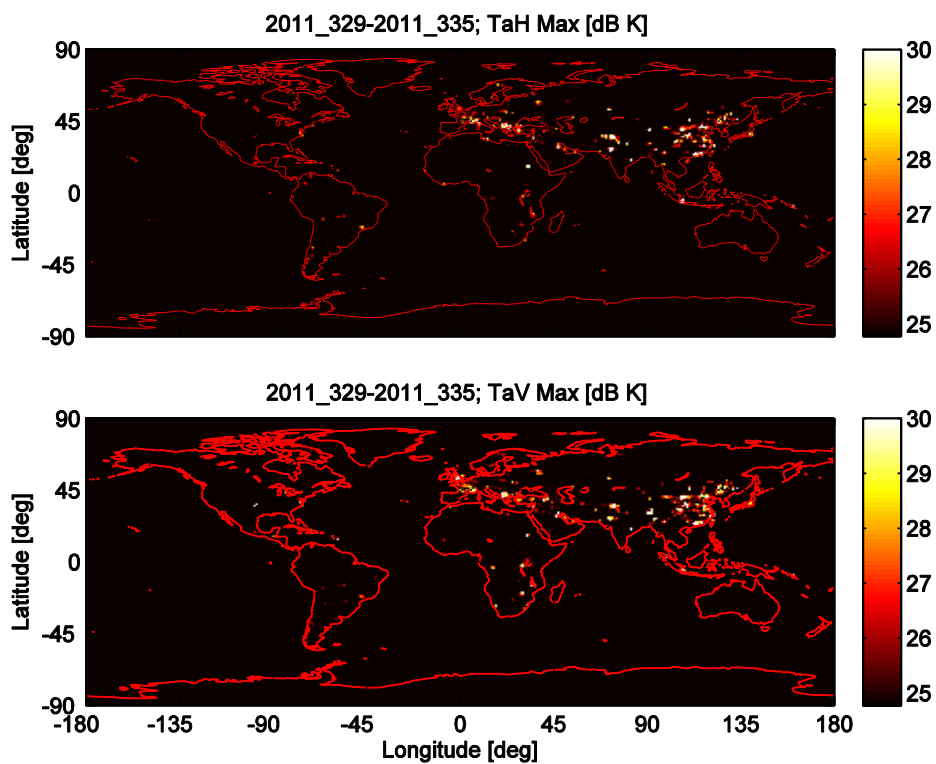
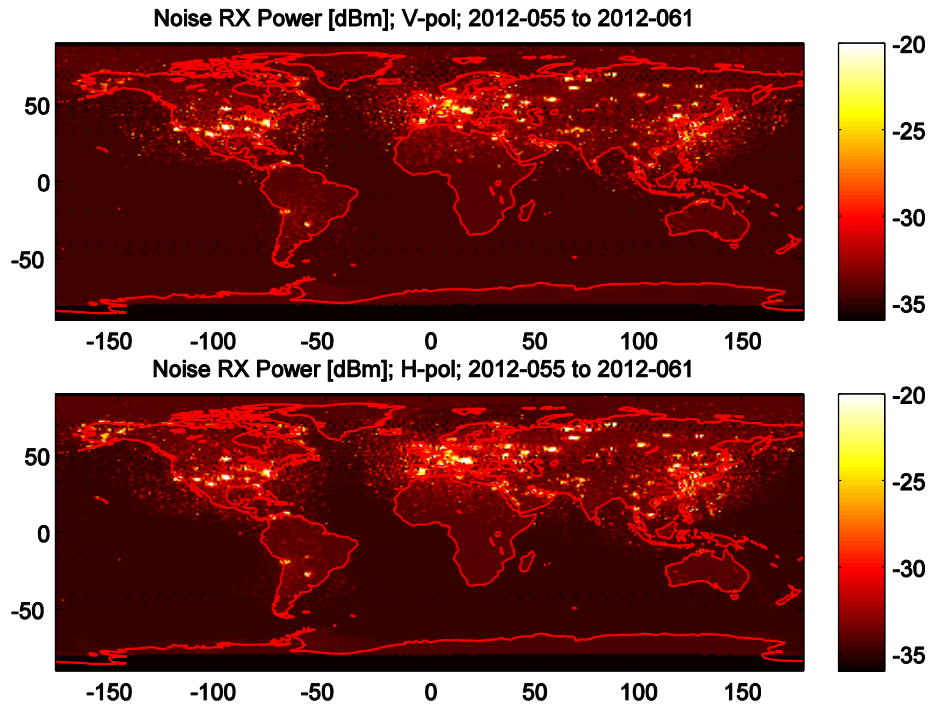


FIGURE 19 (cont.)

Global maps of Aquarius scatterometer and radiometer RFI

e) Aquarius scatterometer receiver noise power 2012-055 to 061



f) Aquarius radiometer BT 2012-055 to 061

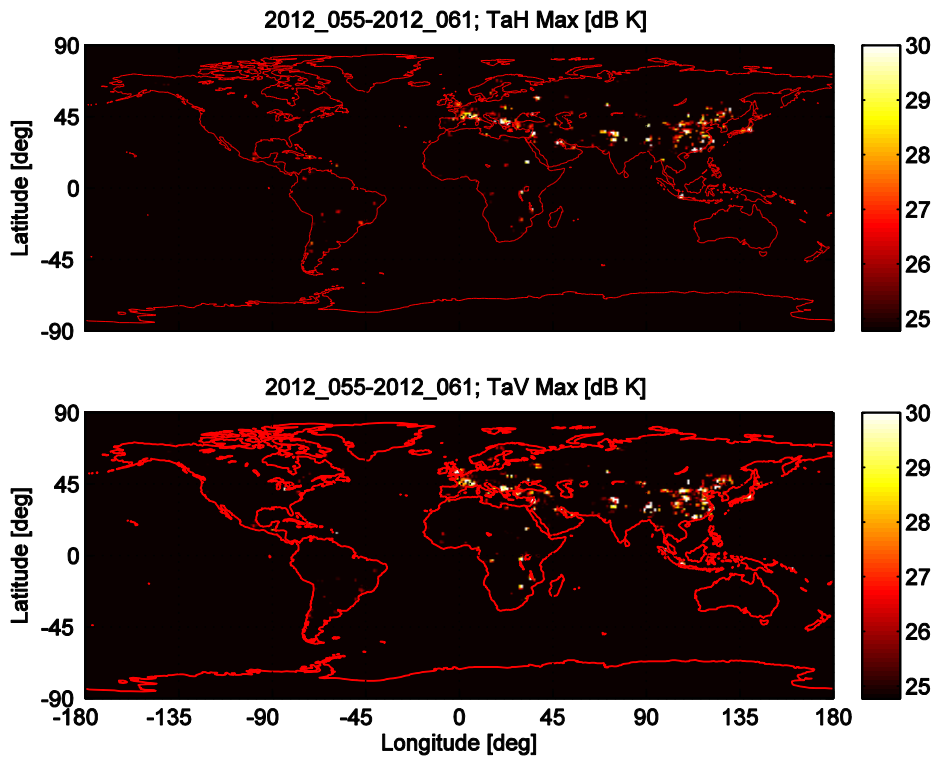
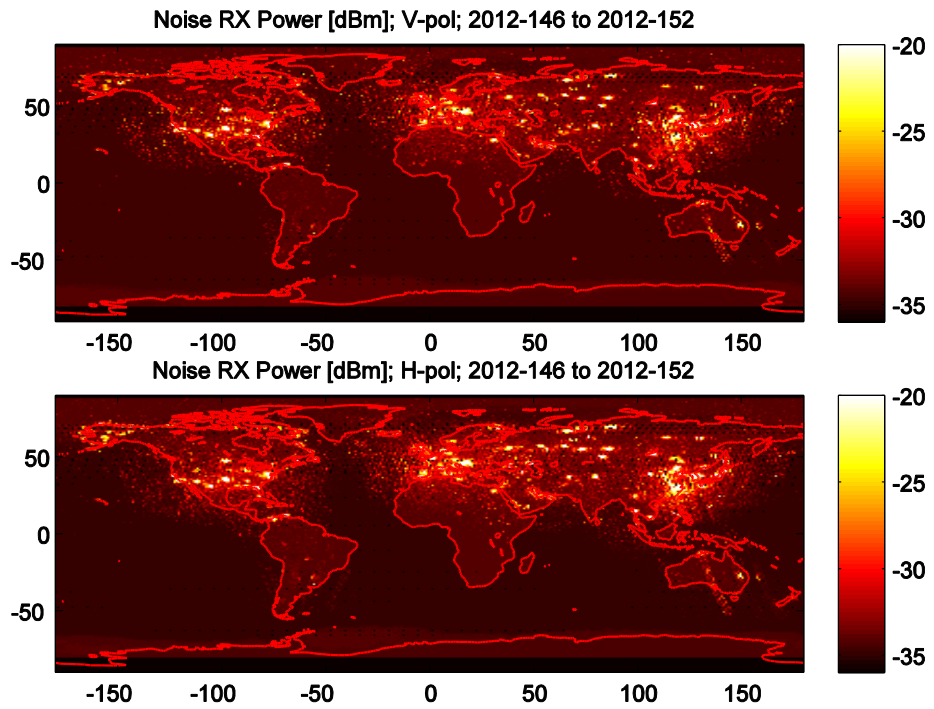




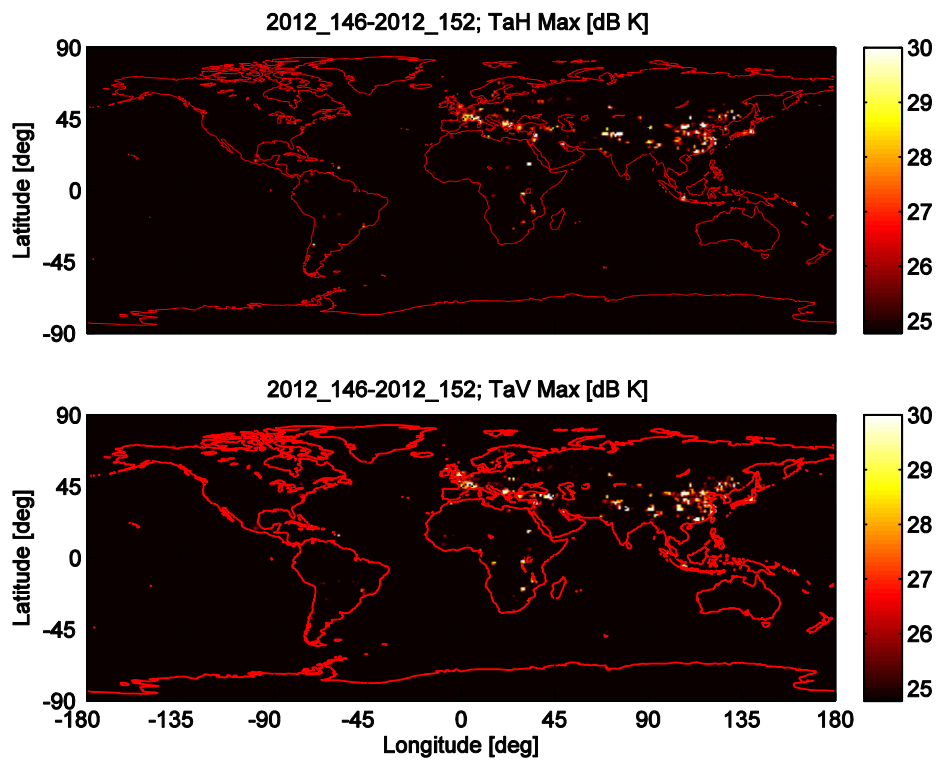
FIGURE 19 (end)

Global maps of Aquarius scatterometer and radiometer RFI

g) Aquarius scatterometer receiver noise power 2012-146 to 152



h) Aquarius radiometer BT 2012-146 to 152



#### **4 Observation of RFI by SMOS radiometer in the passive band 1 400-1 427 MHz**

The Soil Moisture and Ocean Salinity (SMOS) mission is a joint program led by the European Space Agency (ESA) with participation of the Centre National d'Etudes Spatiales (CNES) in France and the Centro Para el Desarrollo Tecnológico Industrial (CDTI) in Spain. Its main scientific objective is to observe soil moisture over land and sea surface salinity over oceans. SMOS was launched on November 2, 2009 and became operational in May 2010. The mission has been recently extended until 2017. The main scientific objective of SMOS is to observe soil moisture over land and sea surface salinity over oceans. As soon as SMOS data analysis began, it became clear that RFI is distributed worldwide, in particular over large parts of Europe, China, Southern Asia, and the Middle East. The RFIs have impact in the data quality of both, the soil moisture and the sea surface salinity observations, and is leading to significant amounts of data being discarded since they are unusable by scientific users and operational agencies.

##### **4.1 Description of SMOS radiometer**

SMOS has a single payload on board, which consists on a microwave imaging radiometer using aperture synthesis (MIRAS). MIRAS is a passive microwave 2-D interferometric radiometer comprising a central structure, the hub (1.3 m diameter), and 3 deployable arms extending up to 8 m in diameter. Each arm comprises eighteen L-Band receivers, complemented by a further twelve receivers, and three noise injection radiometers (NIR) in the central hub. In total, the MIRAS payload comprises 69 antenna elements.

SMOS measures the brightness temperature emitted from the Earth at L-band over a range of incidence angles (0 to 65°) across a swath of up to 1 400 km with a spatial resolution of 35 to 50 km. The SMOS brightness temperatures are the so-called Level 1 data products, based on which two level 2 data products are retrieved, namely the Level 2 soil moisture and Level 2 ocean salinity. A key requirement in the design of the receivers was the rejection of signals outside the 1 400-1 427 MHz passive band. The SMOS RF band pass filter response actually implemented on board the satellite is shown in Fig. 20. The centre frequency of the filter is 1 413.5 MHz with a -3 dB bandwidth of 19 MHz. Furthermore, additional rejection is achieved due to the overall receiver selectivity response (complete receive chain): 32 dB at 1 400 MHz and 77 dB at 1 397 MHz.

The instrument topology and imaging geometry for nominal measurement mode is shown in Fig. 21. The satellite control utilises local normal pointing and yaw steering. The normal to the face of the instrument (the  $+x_A$  axis) is offset from the nadir direction by a 32-degree tilt in the orbital plane (i.e. a pitch rotation). Yaw steering ensures that the trajectory of all targets is parallel to the ground track velocity vector. Strong RFI can affect measurements thousands of kilometers away from the antenna source, as can be shown in Fig. 22.

FIGURE 20  
SMOS RF filter response

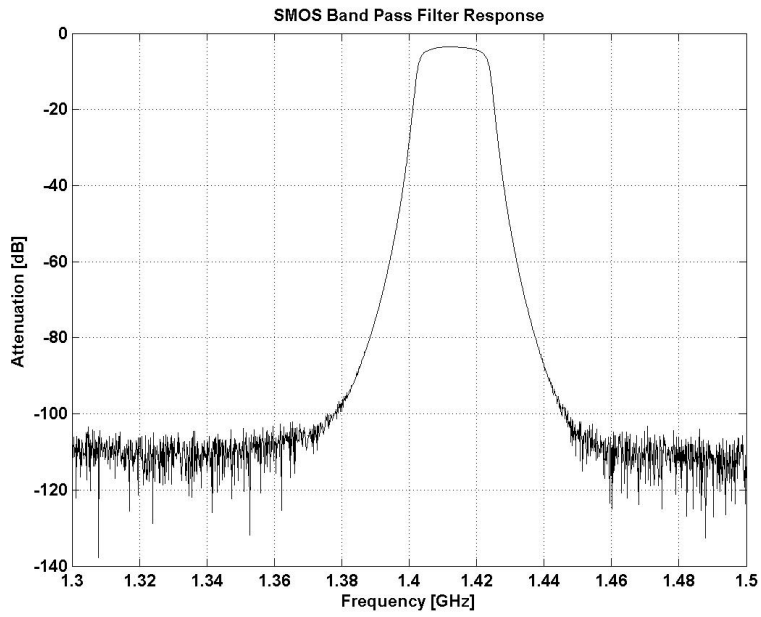


FIGURE 21  
Geometry of SMOS observation mode

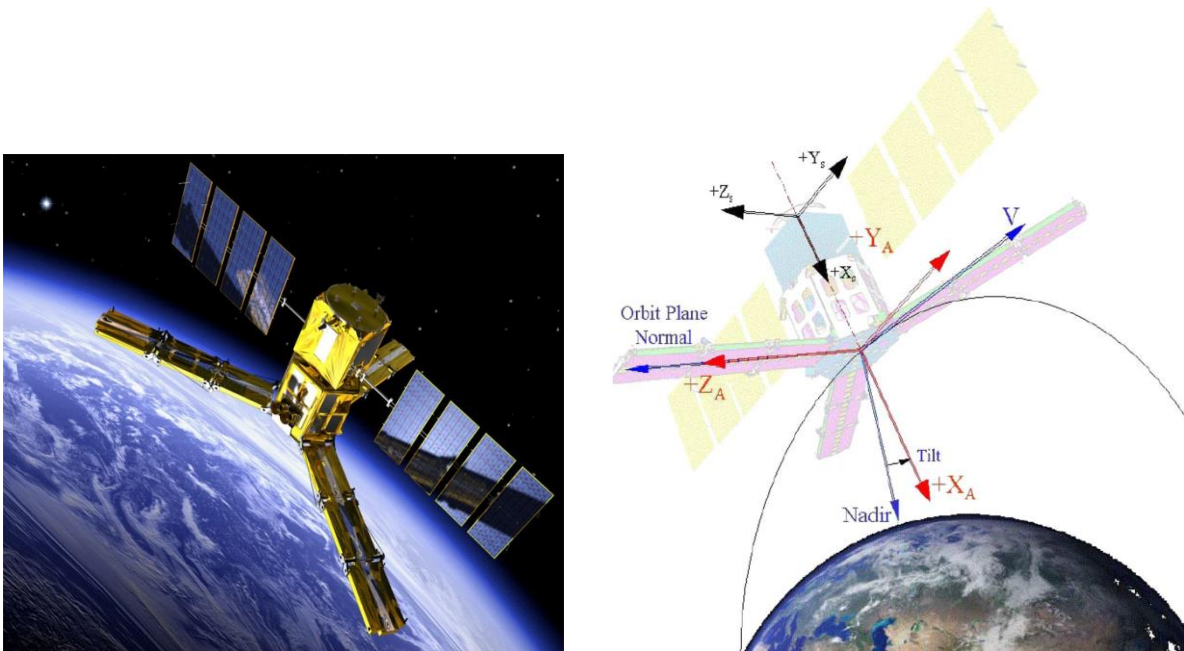
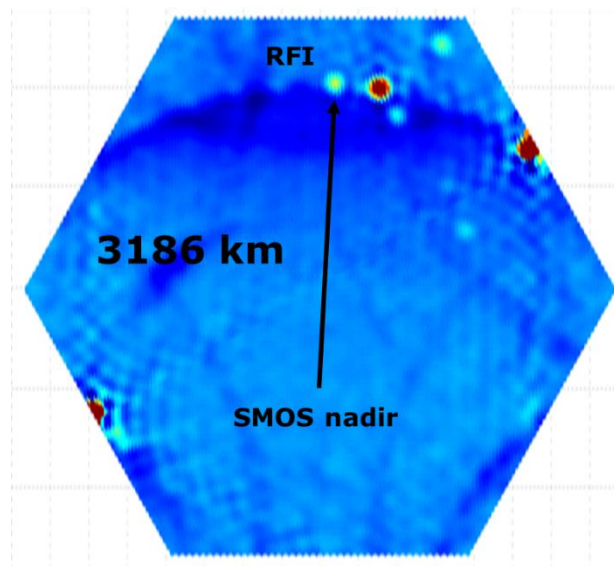

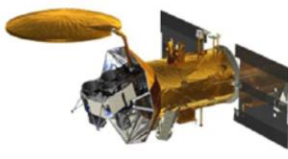


FIGURE 22  
SMOS field of view



The characteristics of SMOS and Aquarius radiometers are very different, however both systems are impacted of the RFI scenario worldwide. The table below summarises the main differences:

SMOS	Aquarius
<ul style="list-style-type: none"> <li>• Launched Nov 2009</li> <li>• 2D-synthetic aperture               <ul style="list-style-type: none"> <li>• Multiple incidence angles at every location [0°-65°]</li> </ul> </li> <li>• Sun Synchronous orbit with an ascending orbit of 6:00 AM</li> <li>• Spatial resolution 40 km</li> <li>• Swath – 1400 km</li> <li>• 3 day global coverage</li> </ul>	<ul style="list-style-type: none"> <li>• Launched June 2011</li> <li>• Real aperture               <ul style="list-style-type: none"> <li>• Three incidence angles of 29.36°, 38.49°, 46.29°</li> </ul> </li> <li>• Sun Synchronous orbit with an descending orbit of 6:00 AM</li> <li>• Spatial resolution 100 km</li> <li>• Swath – 350 km</li> <li>• 7 day global coverage</li> <li>• 7 day exact repeat</li> </ul>
	

Source: Inter-Comparison of Aquarius and SMOS Brightness Temperature Observations, by Rajat Bindlish, Thomas Jackson, Tianjie Zhao, Gary Lagerloef, David Le Vine, Simon Yueh, and Yann Kerr. (Nov 6, 2013)

#### 4.2 Approach to improve the SMOS RFI situation

Several strategies have been put in place to improve the RFI scenario observed and to minimise the negative impact in the scientific retrieval worldwide:

- In the short and medium term:

- a) to report the detected RFI sources to the National Spectrum Management Authorities and request for their cooperation to initiate investigations. The Authorities will send their RF monitoring units to the site to localize the RFI source and take the necessary action to cancel or at least mitigate its effect;
  - b) to localize and flag the RFI contamination in the respective Level-1 data product, thus avoiding that this data is used for the retrieval of Level-2 data products;
  - c) to investigate new RFI mitigation algorithms.
- In the medium and long term:
- a) to increase the awareness of the international community about RFI problem for passive sensors and the impact in the scientific return of scientific missions;
  - b) to work within ITU and regional organisations to improve the regulations and tools dedicated to the protection of passive remote sensors in 1 400-1 427 MHz frequency band.

### 4.3 Characterisation of the RFI sources

#### 4.3.1 Type of emissions vs. the RFI strength

The RFI detection included in soil moisture retrieval algorithms allows detecting strong RFI emitters but also weaker sources. The RFI sources are detected when their BT are outside of the geophysical expectation range. The maximum BT due to natural sources is the physical temperature of the source and the maximum ground temperature ever recorded so far is  $\sim 338$  K ( $65^{\circ}\text{C}$ ). Therefore, BTs values above 338 K indicate that there is a man-made emission in the band.

The RFI emissions can be categorized as low, moderate, strong or very strong:

- **Low RFI emissions** have levels similar to natural sources and are difficult to detect, leading to incorrect physical retrieval.
- **Moderate RFI emissions** are easily detectable but their effects are circumscribed to the on-ground emitter's location. The quality of the data will be negatively affected, with less data available for the retrieval leading to less accuracy. These man-made emissions within the passive band are observed by SMOS as strong point source emissions. See Fig. 23.
- **Strong RFI emissions** influence larger areas through the secondary lobes tails, which need to be discarded for scientific retrieval, thus leading to a significant data loss. See Fig. 24.
- **Very strong RFI emissions** essentially hide the full SMOS field-of-view and can blank out any natural signal over a range of several hundreds of analyses, causing significant loss of data for scientific retrievals. In this respect, there are observed occasional but RFI recurrent flares in Europe that are able to saturate some of SMOS receivers. See Fig. 25.

FIGURE 23

SMOS BT maps showing detection of moderate RFI point source emissions

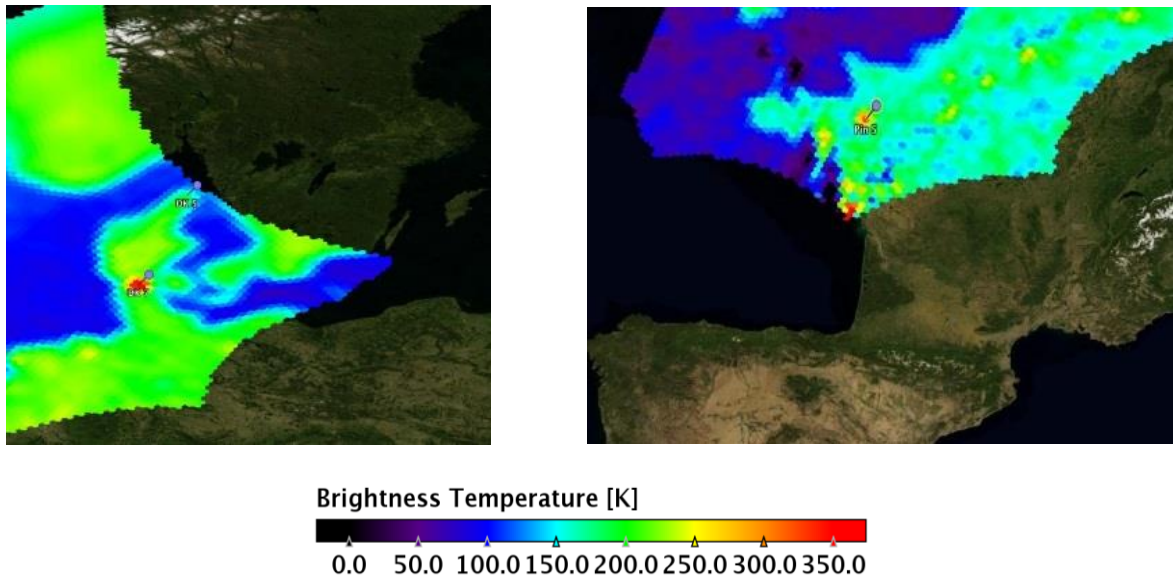


FIGURE 24

SMOS BT maps showing detection of strong RFI emissions

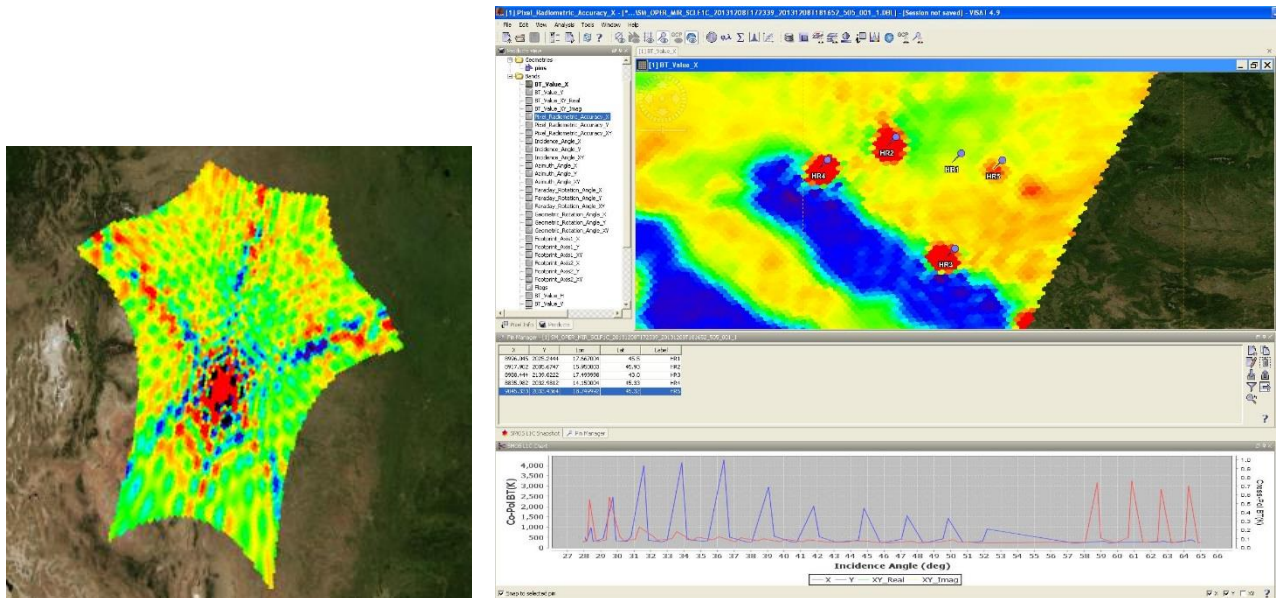
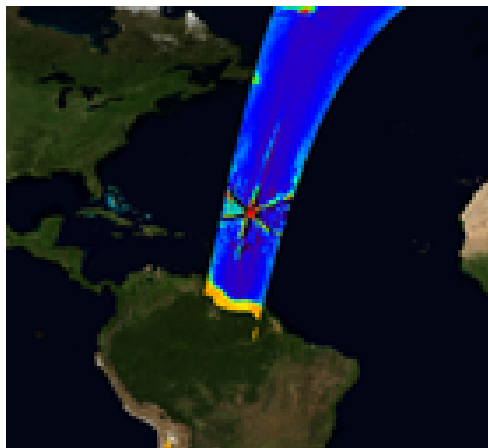
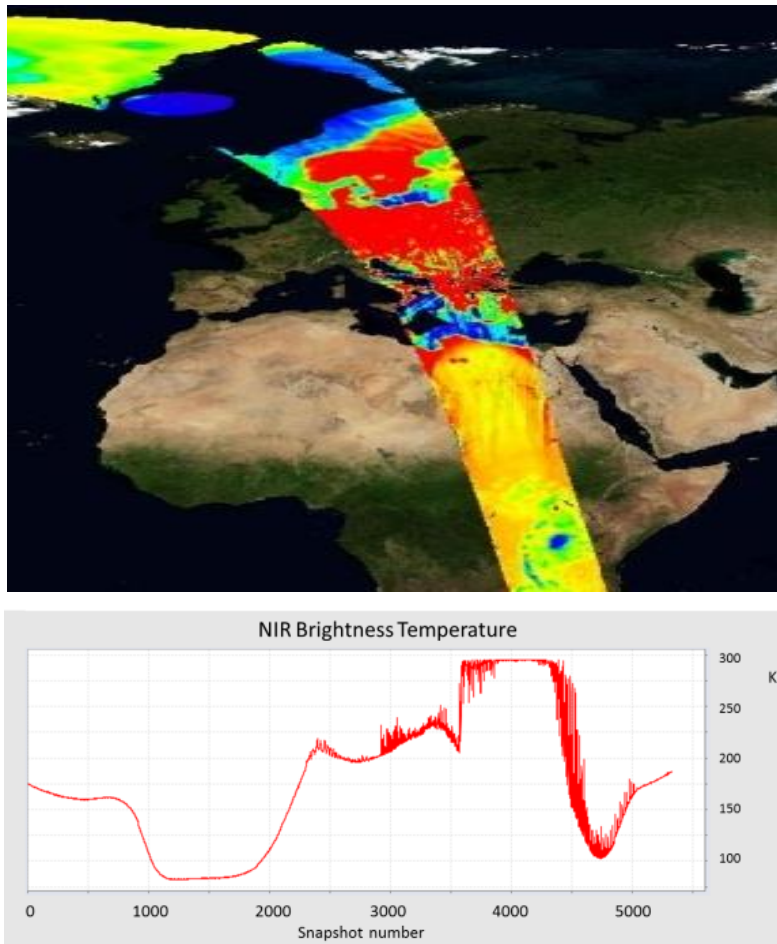


FIGURE 25

SMOS BT maps showing the impact of very strong RFI emissions



#### 4.3.2 Type of emissions vs. the RFI source

The RFI sources can also be grouped into two main categories, depending if the RFI emission is produced by a transmitter operating within the passive band or in the adjacent bands, as it is depicted in Fig. 26.

- **In-band emissions in the protected band.** These RFIs are caused by unauthorized radio links, TV and FM broadcast stations, wireless monitoring cameras, malfunctioning DECT

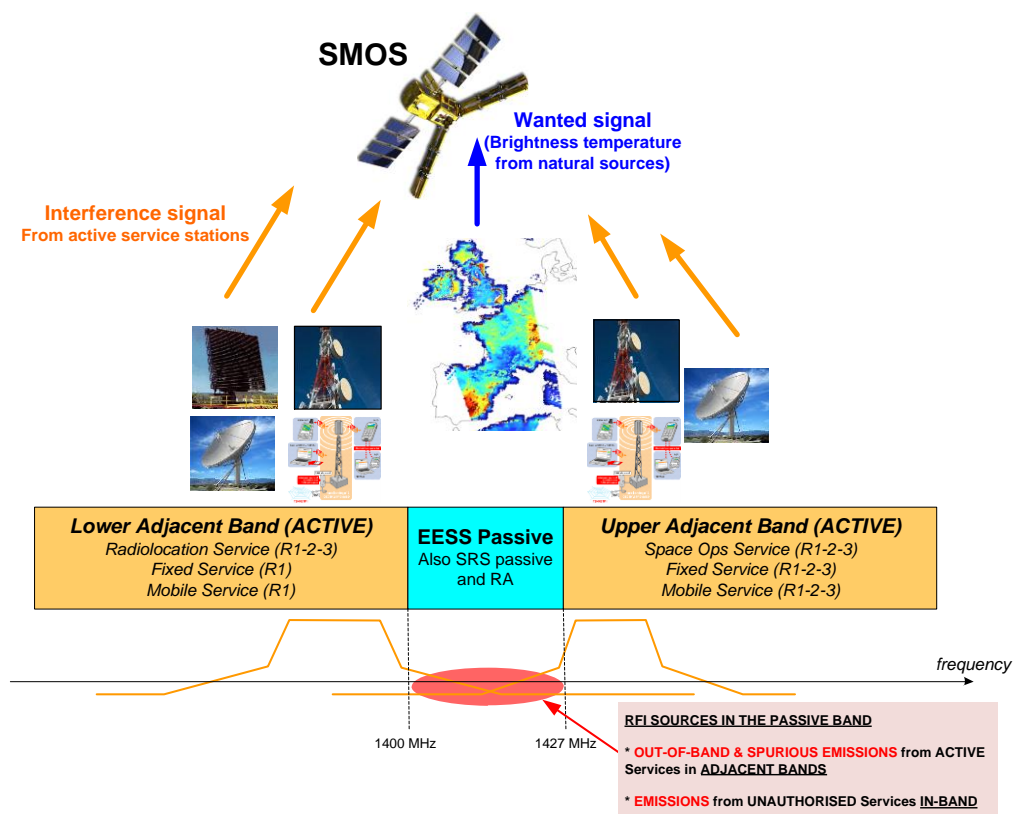
phone terminals, equipment with lack of maintenance whose frequency of operation has drifted over time, etc.

- **Excessive unwanted emissions from systems operating in the adjacent bands.** Typically these interferences are due to excessive out-of-band emissions of radar systems. The spurious emissions of radio link equipment operating in adjacent bands are also a common source of interference.

The type of emission causing the interferences cannot be determined based only on the satellite observations. The feedback received from the National Spectrum Management Authorities is key to be able to better characterise the RFI source and establish some statistics and to further improve the interference detection, mitigation, and cancellation techniques.

FIGURE 26

Graphic representation of EESS allocation and neighbouring services in the 1 400-1 427 MHz



#### 4.3.3 Parameters used to characterise the RFI sources

The analysis of the SMOS observations allows gathering information on the nature of the source causing the RF interference. Typically the following parameters are provided by ESA to the National Spectrum Management Authorities so that investigations can be initiated:

- maximum BT measurement observed of the RFI source;
- geographical location, typically with 5 km accuracy;
- approximate RFI emitter pointing direction (useful to identify directive emissions such as radio links);



- periodicity of the observation (useful to identify possible scanning radar emissions);
- snapshots of BT measurements, RFI brightness temperature maps and RFI probability maps.

#### 4.3.4 Types of maps used to report the RFI situation

There are essentially two sort of maps used to characterise the distribution of RFIs over a region: the brightness temperature maps and the RFI probability maps.

The BT maps provide reliable information about the position and distribution of the RFI sources on ground and are used as part of the RFI detection and geo-location process. The RFI BT maps (see Fig. 27) are produced as a compilation of snapshot images (see Fig. 28). SMOS L1c products provide geo-located measurements of BT. These measurements integrate the radiation received at the satellite every 1.2 s. The SMOS team at ESAC (ESA facilities in Spain) regularly scans these SMOS images and prepare probability maps. Whenever a RFI is detected, a semiautomatic algorithm analyses several SMOS passes over that area. The objective of the algorithm is to estimate, as best as possible, the on-ground location of the RFI and its BT intensity. Even though SMOS spatial resolution (35-55 km) is not very adequate for this purpose, the algorithm relies on the large amount of observations to improve the accuracy of the geographical coordinates of the antenna emitter. Considering that during one pass, each point on-ground is measured several times under different incidence angles (as the satellite moves forward) and that at least two weeks of measurements over that region (i.e., ~10 passes) are used to infer the RFI position, the final accuracy of this technique is better than 5 km in the majority of the cases (see Fig. 29).

See [http://www.esa.int/About\\_Us/ESAC/ESAC\\_SMOS\\_Data\\_Processing\\_Ground\\_Segment](http://www.esa.int/About_Us/ESAC/ESAC_SMOS_Data_Processing_Ground_Segment)

The RFI probability maps indicate the probability that a certain position on ground will be affected by the contamination of any of the source. The Level-2 soil moisture processor allows retrieving statistical information of the SMOS pixels affected by RFI and this data can be presented as probability maps of RFI occurrences during a certain period of time. The RFI detection included in soil moisture retrieval algorithms allows detecting strong emitters but also weaker sources. The geophysical expectation range uses variable thresholds dependent of the minimum/maximum physical earth surface temperature within the antenna footprints. The basis of the probability maps is to count the number of BTs considered as contaminated per pixel and orbit and to accumulate counters. The colour bar ranges from red (100%), indicating that RFIs are always present and means that no BT measurements were kept at all during 15 days, to deep blue, indicating none to very low probability and thus almost all BT measurements were kept as usable for retrieval. Intermediate values indicate a high proportion of RFI presence but do not tell when the occurrences appeared within the time window considered. A probability of 50% (green) is equally obtained by 7.5 days of continuous strong emissions followed by 7.5 days of no emission at all, or by alternating one day with strong RFI followed by one day RFI off or any other combinations.

FIGURE 27  
SMOS RFI BT map of Europe (August 2010)

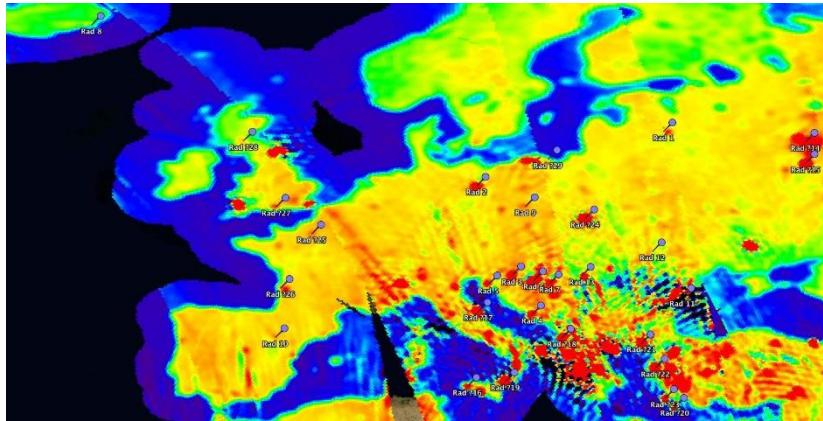


FIGURE 28  
SMOS RFI BT snapshot (Nov. 2012)

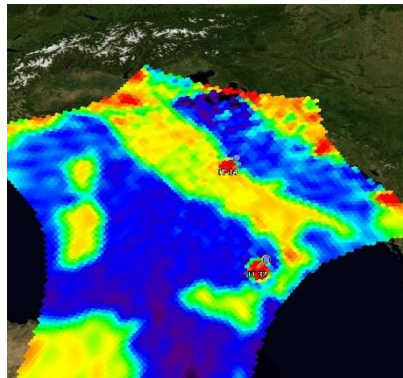
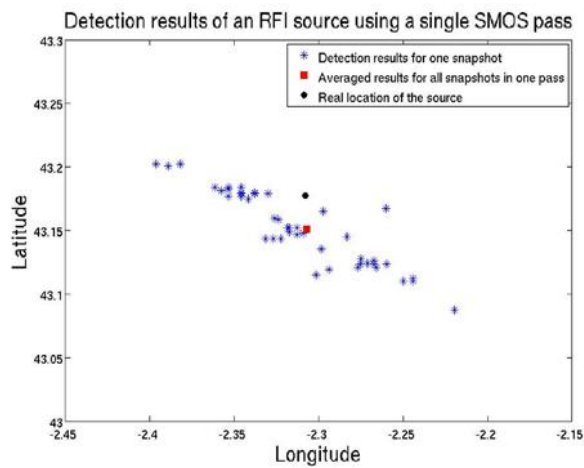


FIGURE 29  
Example of SMOS RFI detection (*credits: R. Oliva, ESA ESAC*)

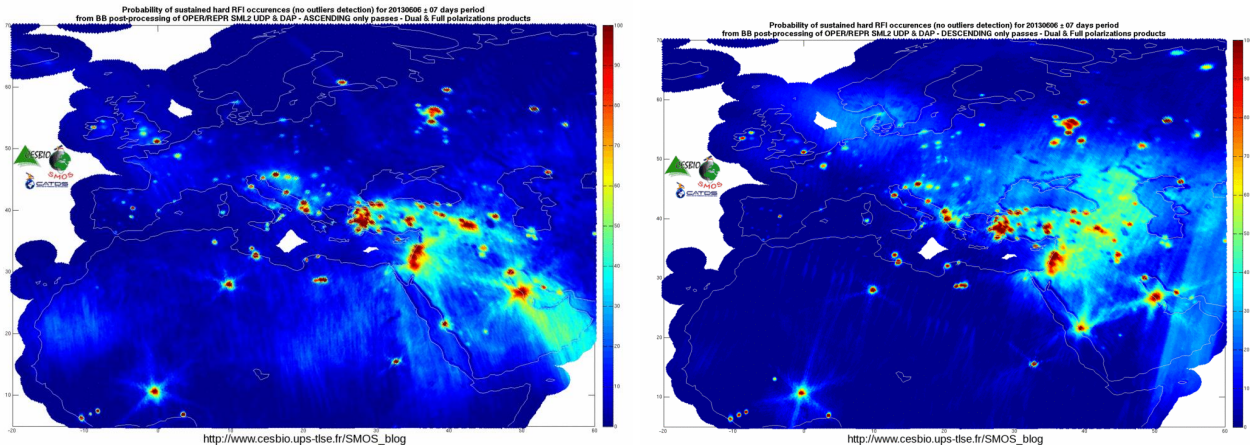


The RFI probability maps are prepared regularly by the SMOS team at CESBIO (CNES, France). Figure 30 shows the RFI probability maps for ascending and descending passes in Europe in June 2013.

A full catalogue of RFI probability maps since the beginning of the mission is available at the site: [http://www.cesbio.ups-tlse.fr/SMOS\\_blog/smos\\_rfi/](http://www.cesbio.ups-tlse.fr/SMOS_blog/smos_rfi/)

FIGURE 30

Europe RFI probability maps for a 2-weeks window in June 2013 (*credits: P. Richaume, CESBIO*)



(*ascending passes*)

(*descending passes*)

#### 4.4 Global survey of RFI as observed by SMOS radiometer

The overall situation of SMOS RFI as observed in September 2014 is presented in a worldwide inventory depicted in Fig. 31. The position of an RFI is obtained averaging all its localizations made within the validity period. The colour of each RFI is proportional to its averaged BT. As RFI BTs are the sum of the natural thermal noise and the artificial emissions, BT lower than 300 K are not represented. The maximum of the colour-bar has been fixed at 10 000 K in all images for consistency, but in many cases stronger RFI are present. The size of each point is proportional to RFI persistence in SMOS data, i.e. the number of times the RFI was detected. Because of SMOS polar orbit, RFI at high latitudes tend to be larger, since these latitudes are observed more often, with indication of the strength (BT) for the sources.

The RFI probability maps for descending passes during two weeks period in 2014, 2010 and 2013 are presented in Figs 32, 33 and 34, respectively.

FIGURE 31

Worldwide inventory of RFI observed by SMOS from 6 to 20 September 2014 (credits: CESBIO)

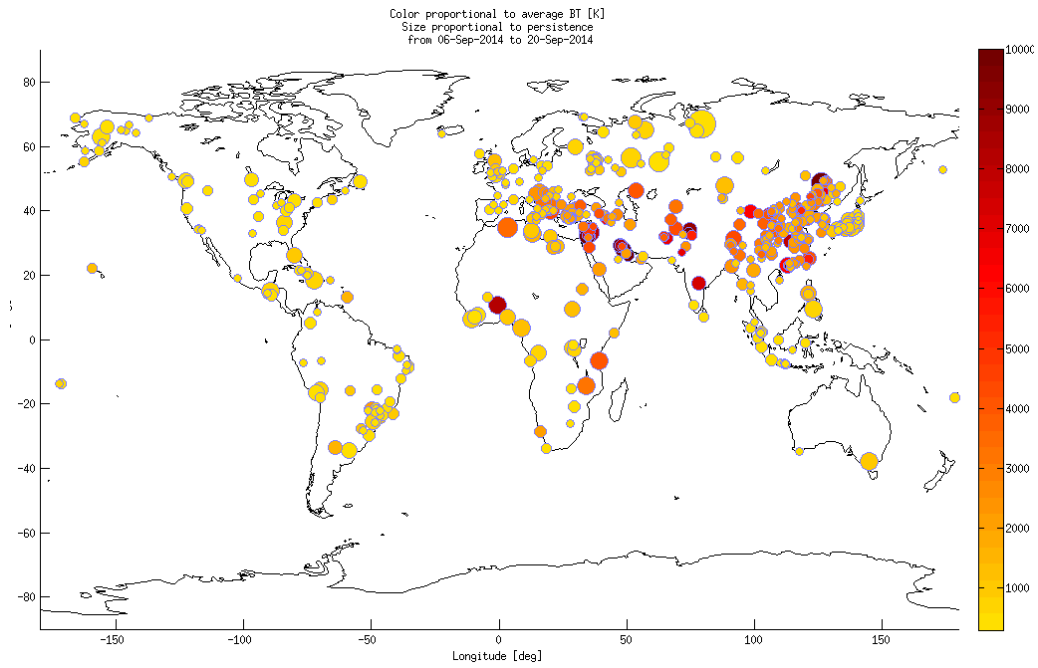


FIGURE 32

SMOS RFI probability for descending passes from 1 to 14 September 2014 (credits: CESBIO)

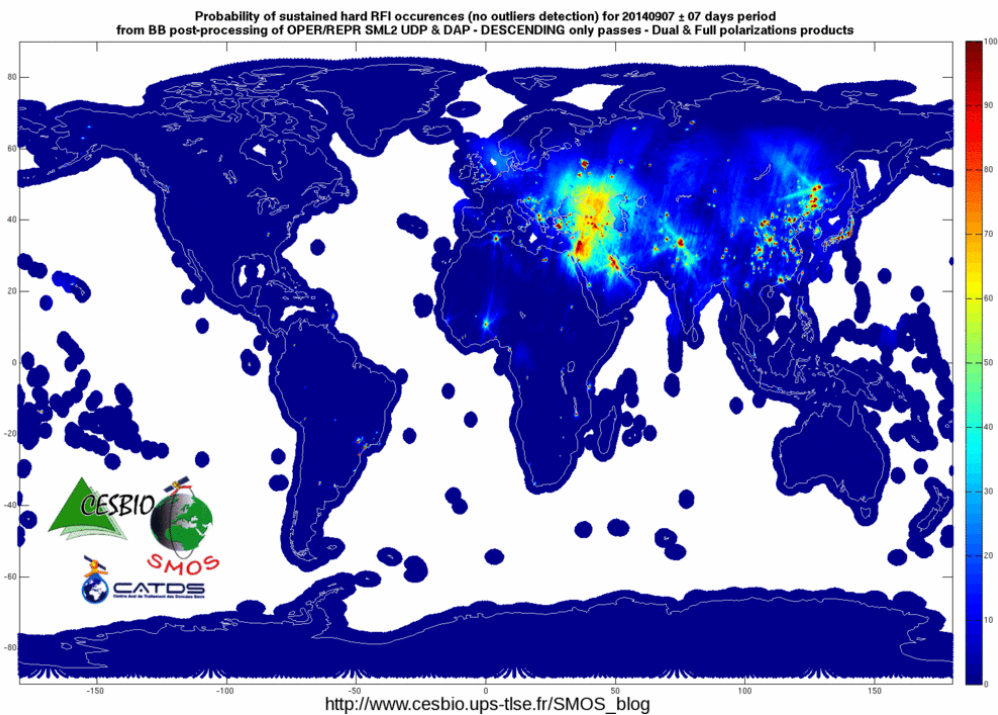


FIGURE 33

SMOS RFI probability for descending passes from 14 to 28 January 2010 (credits: CESBIO)

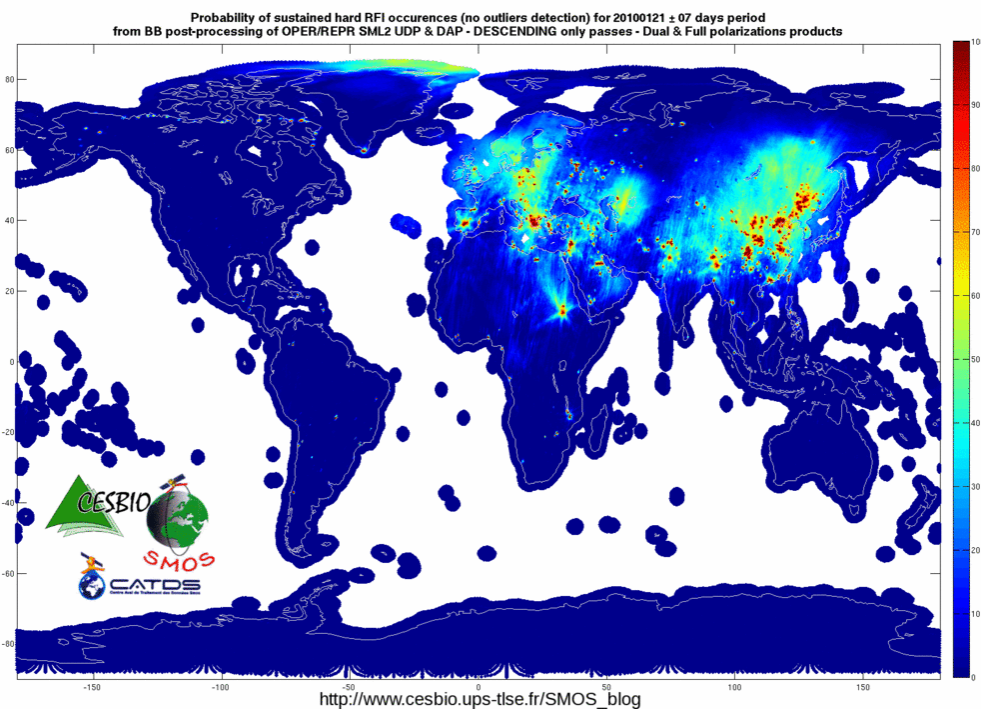
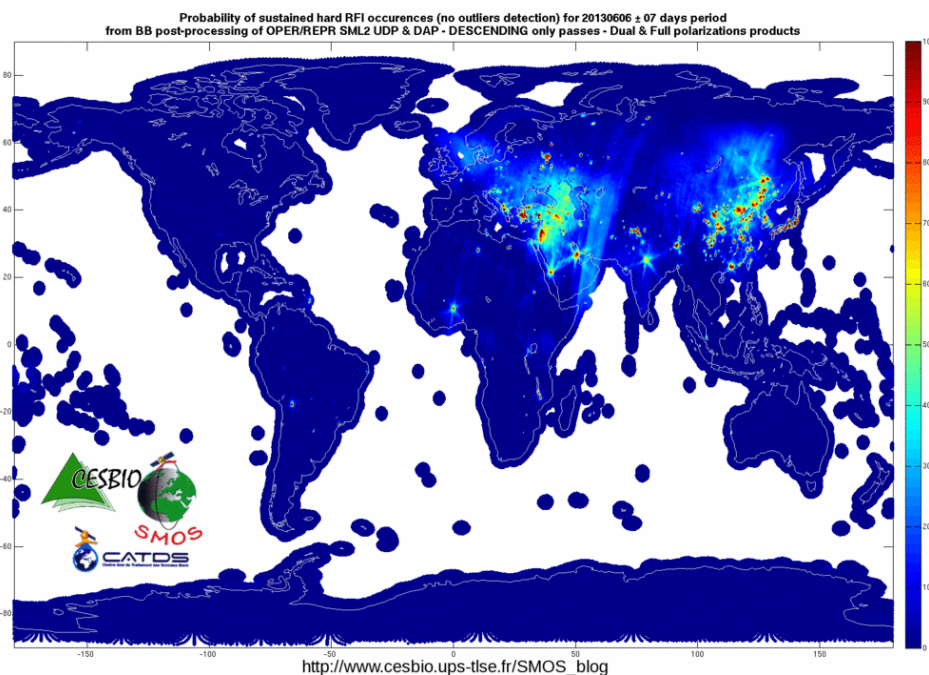


FIGURE 34

SMOS RFI probability for descending passes from 30 May to 13 June 2013 (credits: CESBIO)



#### 4.5 Worldwide evolution of RFI occurrences

More than 3 000 RFI occurrences have been observed worldwide. In some cases the interference is only observed during a limited period of time. The approach followed in the investigation of RFIs has been to focus the efforts in the RFI cases that are observed regularly, giving priority to the investigation of those interferences more disturbing for the scientific benefit of the mission.

ESA has contacted 44 administrations worldwide, as RFI occurrences are distributed in all regions. In general there has been a good cooperation of the spectrum management authorities of most countries, in particular in Europe but also in Canada, United States of America and Japan. Unfortunately this is not always the case and some administrations have not taken any action to investigate the RFI cases reported in their territory.

As of August 2014, up to 687 constant RFI have been detected and 362 RFIs (52%) have been identified and switched off.

Most RFI sources are detected over Asia and Middle-East, as presented in Fig. 35. The overall situation is slowly improving. However, in some cases it has been observed that very strong RFIs may be masking other RFI sources underneath, therefore the total number of RFIs detected is increasing and the radiometer measurements over the area remain disturbed by interference.

As a response to the actions initiated by ESA it has been observed a noticeable improvement in the RFI environment over Europe and North America, and some improvement is also observed over China (see Figs 36 and 37). It has been observed recently an important increase of very strong RFI sources in the Middle-East region (see Fig. 32).

FIGURE 35

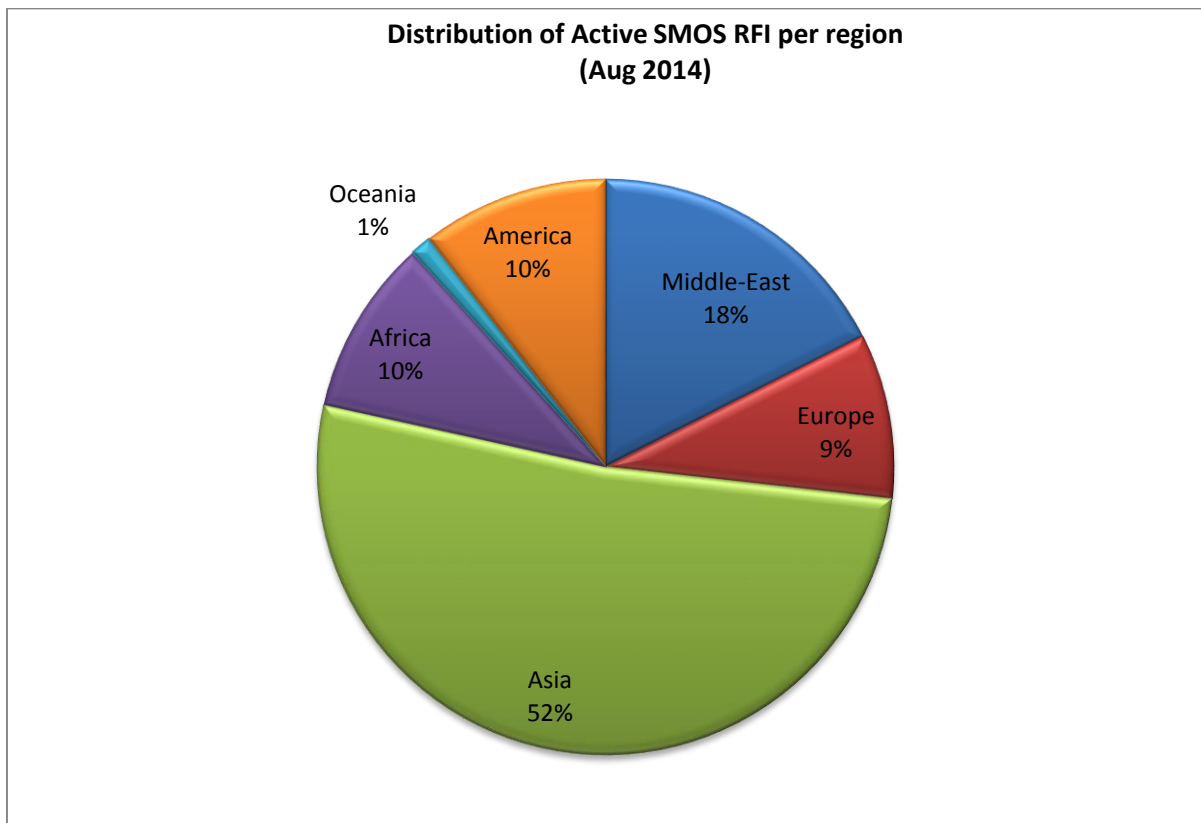


FIGURE 36

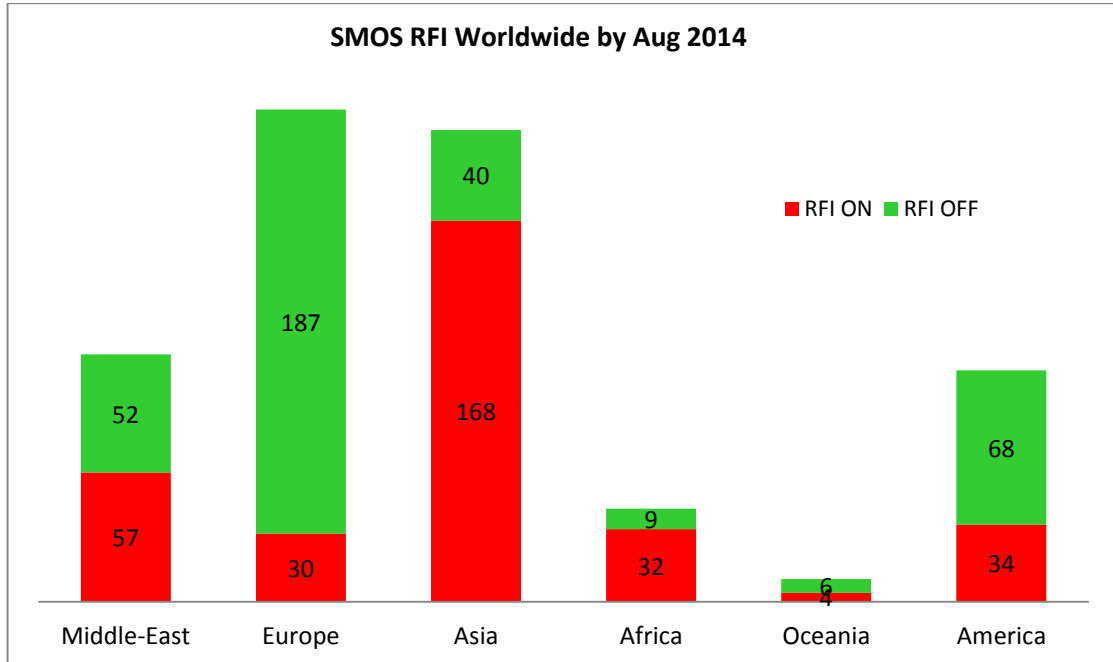
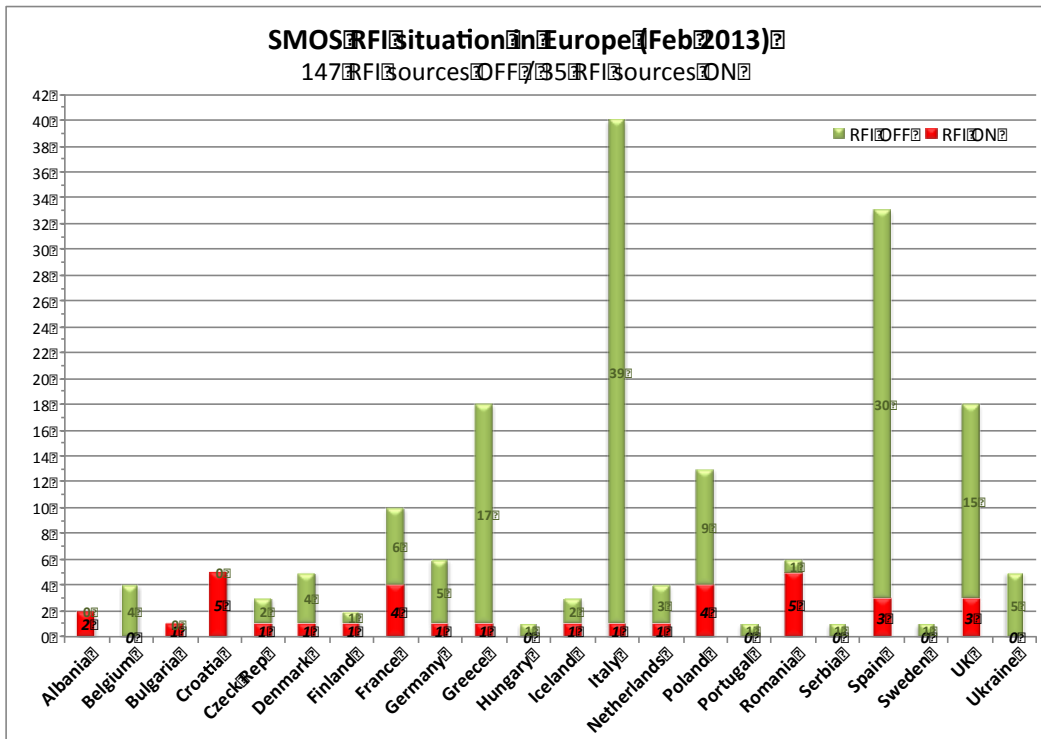


FIGURE 37

Overview of the number of RFI switched off over Europe



### Examples of the evolution of RFI situation in different regions

- A significant improvement has been observed in North America following the refurbishment of several radar systems in Canada. The cooperation of the Canadian authorities to investigate this RFI case and then to upgrade the radar network to reduce the level of unwanted emissions was very important. This improvement had impact not only in the soil moisture measurements but also in the sea salinity monitoring in the arctic areas. See Fig. 38.
- In some cases it has been observed sudden increase in RFIs in areas that before were free of RFI. This is the case of several very strong RFI sources detected in Africa and South America. These RFIs are observed as *point source emissions*.
- A sudden RFI increase, observed as *extended RFI source emissions* has been observed over Japan since Sept. 2011 extended over main urban areas. The Spectrum Monitoring Authorities in Japan are very cooperating and the RFI investigation of this case is on-going. See Fig. 39.
- There have been some cases in which a single RFI source could blind the instrument and caused the loss of data over central Europe for several months. The cause was due to high power emissions from an old radar system operating very close to 1 400 MHz. The National authorities that studied this case took action and the case could be solved. See Fig. 40.
- The support of the administrations is very important to improve the RFI situation, as solved in the examples presented in Fig. 41.

FIGURE 38

Evolution of SMOS RFI in North America following the refurbishment of the L-Band radars

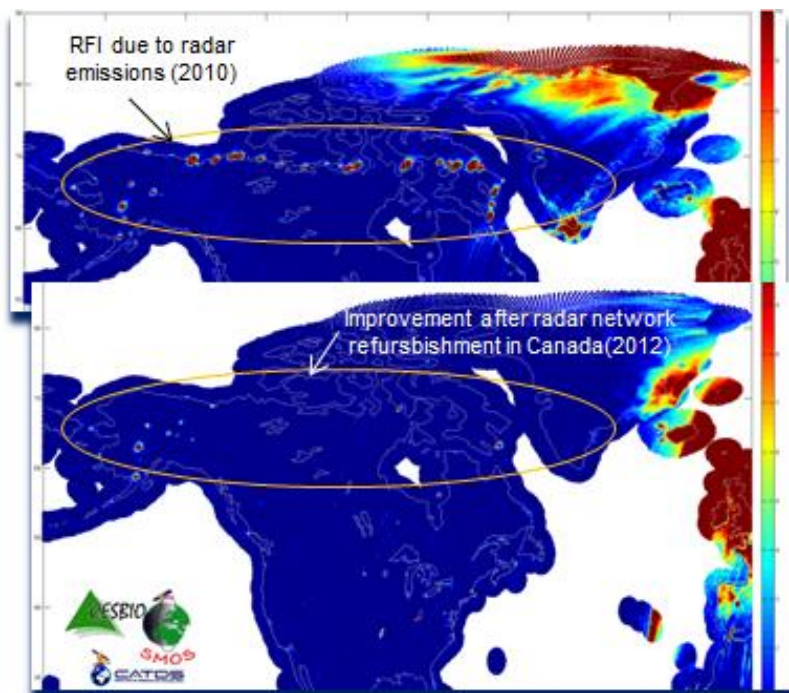




FIGURE 39  
Evolution of SMOS RFI over Japan in September 2011

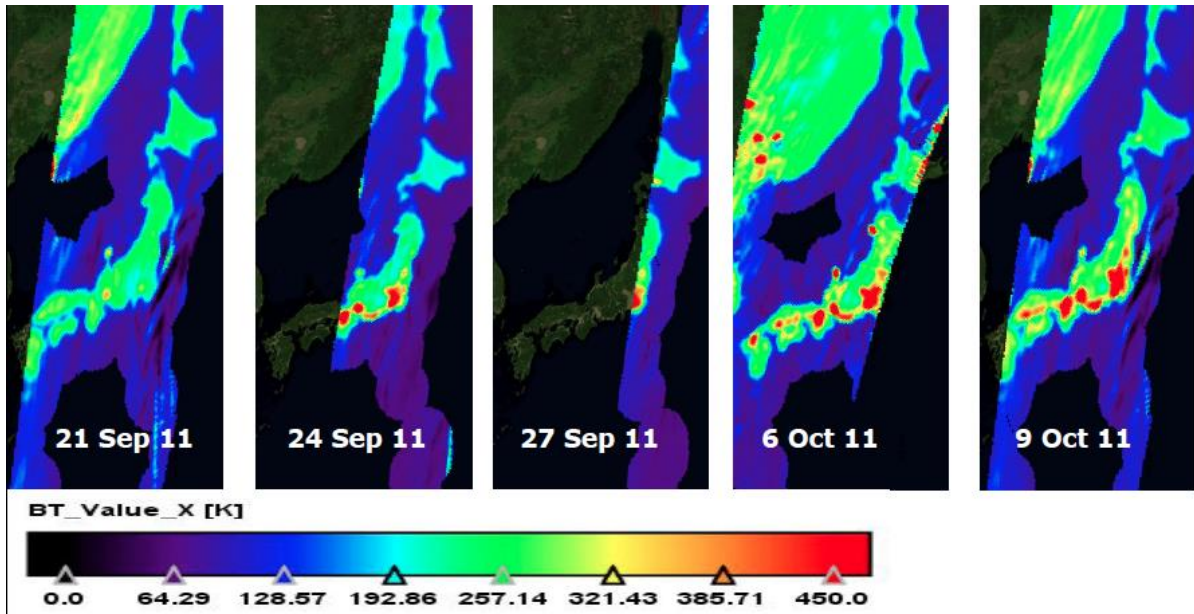


FIGURE 40  
Example of RFI case due to high unwanted emission levels from a radar system

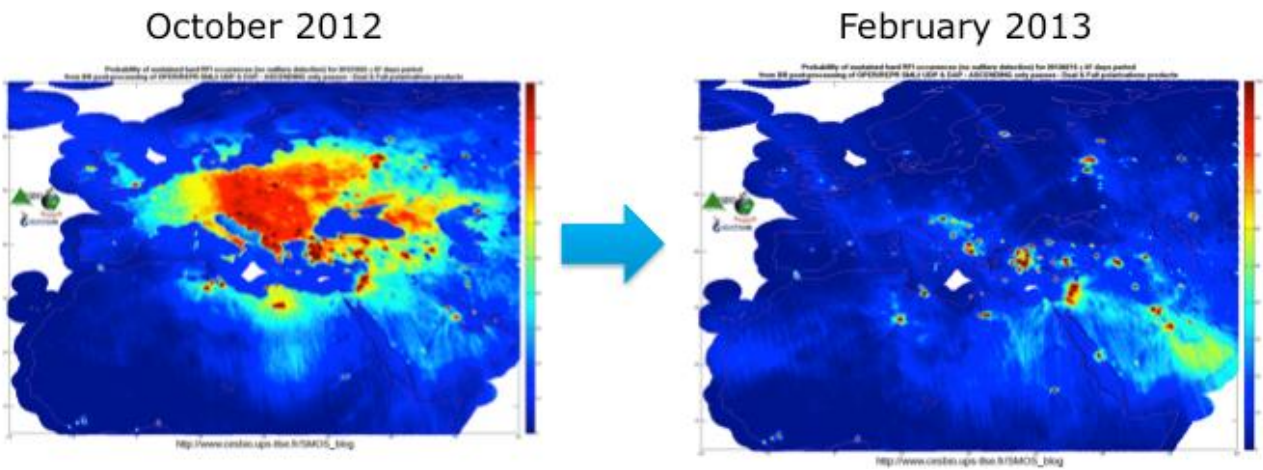
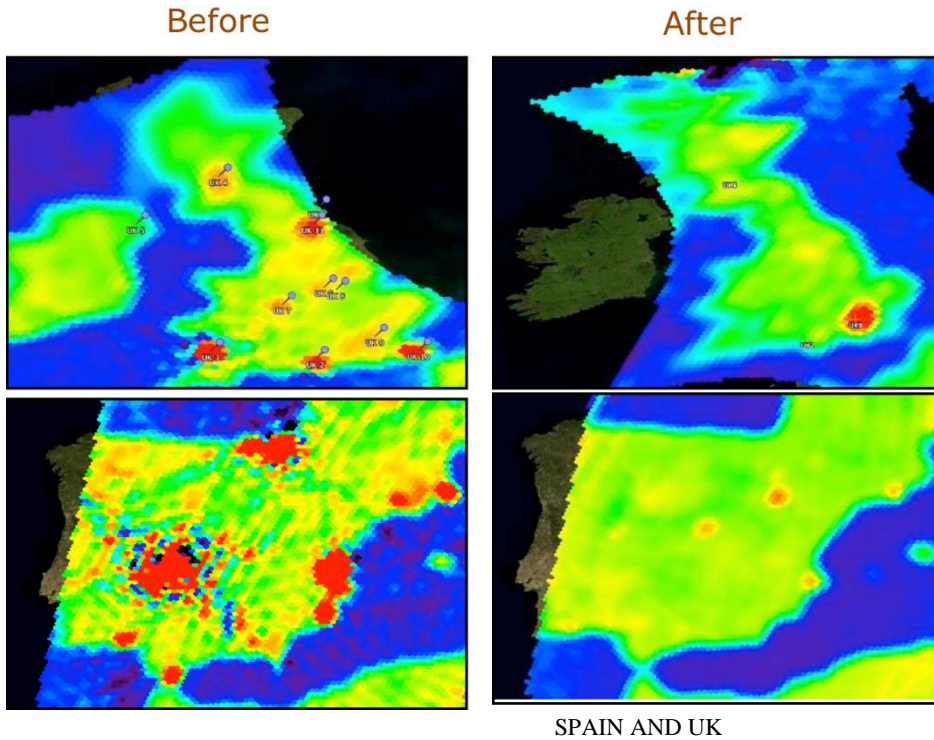


FIGURE 41

Example of RFI case successfully solved thanks to the cooperation of the Spectrum Management Authorities of different countries



## 5 Summary of observed RFI and RFI source analysis

Within this document have been presented RFI as observed globally by the Aquarius scatterometer at 1 260 MHz and by the Aquarius and SMOS radiometers at 1 413 MHz. A comparison of observations is given for the same 7 day period in global maps for both the Aquarius scatterometer and radiometer. Global maps of observed RFI for the SMOS radiometer are also given. Examples are given of how these RFI observation data by the Aquarius scatterometer can be used for RFI source analysis.

It is essential to protect the passive band 1 400-1 427 MHz from both prohibited in-band and excessive unwanted emissions. While the solution of the RFI due to prohibited in-band emissions can be achieved with the cooperation of the national authorities, the solution of the excessive unwanted emissions problem requires regulatory action and compliance with the levels adopted in Resolution **750 (Rev.WRC-12)**. This effort has to be continued and intensified by raising concern among the different administrations.

---